Release of SOS2 kinase from sequestration with GIGANTEA determines salt tolerance in *Arabidopsis*

Woe-Yeon Kim,[1] Zahir Ali, [1] Hee Jin Park, [1] Su Jung Park, [1] Joon-Yung Cha, [1] Javier Perez-Hormaeche,[2] Francisco Javier Quintero, [2] Gilok Shin, [1] Mi Ri Kim, [1] Zhang Qiang, [1] Li Ning,[1] Hyeong Cheol Park, [1] Sang Yeol Lee, [1] Ray A. Bressan, [1,3,4] Jose M. Pardo, [2] Hans J. Bohnert, [1,4,5] Dae-Jin Yun[1]

[1]Division of Applied Life Science (BK21 Program), Plant Molecular Biology and Biotechnology Research Center, Graduate School of Gyeongsang National University, Jinju 660–701, South Korea; [2]Instituto de Recursos Naturales y Agrobiologia, Consejo Superior de Investigaciones Cientificas, 41012 Sevilla, Spain; [3]Department of Horticulture and Landscape Architecture, Purdue University, West Lafayette, IN 47907, USA; [4]College of Science, King Abdulaziz University, Jeddah 21589, Saudi Arabia; [5]Departments of Plant Biology and of Crop Sciences, University of Illinois at Urbana-Champaign, Urbana, IL 61801, USA.

These authors (W.Y. K., Z. A., H.J.P.) contributed equally to the work.

Correspondence and requests for materials should be addressed to D.J.Y. (E-mails: djyun@gnu.ac.kr)

Authors declare no competing financial interests

Abstract

Environmental challenges to plants typically entail retardation of vegetative growth and delay or cessation of flowering. Here we report a link between the flowering time regulator, GIGANTEA (GI), and adaptation to salt stress that is mechanistically based on GI degradation under saline conditions, thus retarding flowering. GI, a switch in photoperiodicity and circadian clock control, and the SNF1-related protein kinase SOS2 functionally interact. In the absence of stress, the GI:SOS2 complex prevents SOS2-based activation of SOS1, the major plant Na^+/H^+-antiporter mediating adaptation to salinity. GI over-expressing, rapidly flowering, plants show enhanced salt sensitivity, whereas *gi* mutants exhibit enhanced salt tolerance and delayed flowering. Salt-induced degradation of GI confers salt tolerance by the release of the SOS2 kinase. The GI-SOS2 interaction introduces a higher order regulatory circuit that can explain in molecular terms, the long observed connection between floral transition and adaptive environmental stress tolerance in *Arabidopsis*.

Introduction

Salt stress in plants includes an osmotic component that can lead to desiccation as the external osmotic potential declines with increasing salt concentrations, as well as a metabolic component as the influx of Na^+ disturbs signaling pathways, protein stability and biochemical reactions[1]. All plants can activate defense mechanisms whose complexity and amplitude depend on genetic complexity and allele structure and to some degree also on the memory of prior salt stress episodes[2]. Although many salinity stress defense genes and pathways have been outlined[2,3], the Salt Overly-Sensitive (SOS) pathway that appears to present a first line of defense has emerged as singularly important in studies using *Arabidopsis thaliana*.

Salt stress can elicit growth reduction by ABA- and GA-mediated (DELLA-dependent) signaling that extends the vegetative phase and inhibits flowering[4,5,6], but the precise mechanism remains unknown. This growth restraint is active and distinct from salt-induced damage. To curtail salt-induced damage, salt-exposed plants maintain low cytosolic Na^+ concentrations by controlling influx, activating efflux, enhancing intracellular compartmentalization and coordinating tissue distribution of the ion. Efficient efflux of Na^+ is achieved in plants by the plant-specific SOS pathway which re-establishes ion and, in part, water homeostasis after exposure to high salinity[7,8]. Among the three known proteins in this pathway, SOS1 is a Na^+/H^+ antiporter regulated positively by a protein kinase complex comprised of the Ca^{2+} activated protein SOS3 and the kinase SOS2, which phosphorylates SOS1 in response to salinity stress[7,9].

The transition from vegetative to reproductive growth is a key event in the life cycle of plants, constituting a crucial determinant of the reproductive success of the organism[10]. Timing of the floral transition is coordinated by a clock that controls the progression of development through genetic and epigenetic programming[11,12,13]. The floral transition requires triggering the initiation of flowering [14,15], and also involves complex redeployment of a variety of metabolic and biochemical processes[16,17]. A plant's environmental history and physiological status is connected to the timing of floral transition because it affects the prospects of survival and adaptation. Although the observational data are often anecdotal, cause and effect have occasionally become established and their genetic foundation corroborated[18]. Usually however, observations of correlations list participants, but fail to provide molecular genetics or biochemical insights into underlying mechanisms.

Although mutations in genes first classified as regulating flowering time have been repeatedly observed to have pleiotropic effects on plant responses to environmentally activated signals, the biochemical processes involved in these interactions are poorly understood[4,19,20,21]. Here we demonstrate that the flowering time gene *GIGANTEA* (*GI*) is a major component of the salt stress adaptation pathway. Although other roles for GI have been reported[22], it is predominantly associated with the promotion of flowering in long day growth. GI is known to be a key component in the photoperiodic control pathway of flowering[23,24], where it mediates light input to the circadian clock. Our results identify GI as the central module in a pathway that responds to the sensing of salinity stress conditions by delaying the initiation of flowering while

providing stress tolerance. We report that GI is a strong negative regulator of salinity stress tolerance. GI cages SOS2 to the nucleoplasm and cytoplasm under normal growth conditions, but is degraded in response to salt stress. This then frees SOS2 to activate the plasma membrane-localized SOS1 Na^+/H^+-antiporter responsible for the export of sodium ions, which has so far been considered the key plant salt defense mechanism. These results provide a unique insight into a molecular mechanism that connects developmental stage transition and environmental stress tolerance in *Arabidopsis*.

Results

GI integrates salinity stress response and flowering time. In *Arabidopsis,* flowering is induced by exposure to long days, with GI recognized as a key component in the photoperiodic control of flowering[23,24,25,26]. GI regulates the precise timing of expression of *CONSTANS* (*CO*), a transcriptional activator of the floral integrator gene *Flowering Locus T* (*FT*).

To examine whether salinity stress provided a signal that affected the timing information in photoperiodic flowering, we first probed for the effects of elevated salinity on floral transition in *gi* mutants that lack GI functional protein. Under long day conditions, WT phenocopies the *gi* mutant upon salt stress (Fig. 1a and Supplementary Figs. S1, S2). All *gi* mutants flowered later than WT in the absence of NaCl. The flowering time of *gi-1*, *gi-2*, and *gi-201* was unaffected in media containing NaCl. (Fig. 1a,b and Supplementary Figs. S1, S2a,b). *CO* and *FT* transcript levels were remarkably

reduced by salt stress in WT, and their levels were low and not affected further by salt in *gi-1* (Fig. 1c) providing an explanation for the abrogation of NaCl-induced delay of flowering in the *gi-1* mutant. GI thus emerged as a player in orchestrating salt-induced late flowering in *Arabidopsis*.

Salt-induced delay in flowering was completely suppressed in a GI-OX line that constitutively overexpresses *GI*. CO and FT are not reduced in a similar way as in WT, indicating that both the timing and expression level of GI are important for NaCl-induced delay of flowering (Fig. 1a,c and Supplementary Fig. S1).

GI expression is under control of the circadian clock[24,27,28] and the cellular level of GI protein is also subject to diurnal oscillation in part due to its dark-induced proteasomal degradation[29]. To evaluate the nature of the delay in flowering in response to salt treatment, GI protein and mRNA were therefore examined in plants expressing HA-tagged GI (*GI:GI-HA*) at close to WT levels. As shown by qRT-PCR, transcript levels of *GI* were enhanced upon salt treatment (Supplementary Figure S3c). This might suggest that *GI* itself is gated by salt. To test for this possibility, the acute salt response of GI transcript levels was examined by 1hr salt treatments at different times of the day. We observed no significant response in *GI* transcript levels with 1hr salt treatments except for an increase at ZT8, the time point when GI transcript levels peak under control conditions (Supplementary Figure S3d). This suggests that an effect of salt on GI transcripts is indirect. While *GI* transcript level was enhanced, GI protein level was reduced in seedlings upon salt treatment although the diurnal cycling pattern was not affected (Supplementary Fig. S3a,b,c and d). For confirmation, GI protein and mRNA

levels were examined in detached leaves of GI over-expressing plant (*35S:GI-HA*). As in seedlings, the steady-state level of GI protein decreased and *GI* mRNA abundance increased upon salt treatment in a time-dependent manner (Fig. 1d,e). Inclusion of MG132, a proteasome inhibitor, during salt treatment abolished the NaCl-induced decrease in the steady-state levels of GI protein (Fig. 1d,e) indicating GI removal upon salt stress also depends on a functional proteasome complex. Regulated GI protein stability could be transmitted through the status of CO (Fig. 1c) thus causing salt-induced delay in flowering. These results explain why the NaCl-induced delay in flowering time depends on the expression of GI.

Increased Na^+/H^+ exchange activity in *gi-1* plants. We next examined whether GI might have a role in the regulation of salt stress responses by examining the salt-stress response of lines differing in GI activity. WT, *gi-1* and GI-OX lines were grown in soil for two weeks and then treated with 150 mM NaCl every 4 days for 2 weeks. In the absence of salt, soil-grown *gi-1* plants showed improved vegetative and delayed reproductive growth in soil compared to WT (Fig. 2a,b). The *gi-1* plants were more tolerant to NaCl than WT. Conversely, GI overexpressing plants showed reduced vegetative but accelerated reproductive growth in the absence of salt, and were more sensitive to NaCl than WT. (Fig. 2a,b). These results suggest that GI functions as a negative factor interfering with mechanisms leading to salt tolerance.

Exposure of plants to stresses induces reprogramming of the transcriptome that reflects coping mechanisms. The *P5CS1* gene and genes encoding transcription factors of the dehydration responsive element binding protein/C-repeat binding factor

(*DREB/CBF*) family, such as *DREB2A*, are prominent among genes induced by numerous abiotic stresses and are considered as general stress response markers[3,30]. We considered the possibility that GI regulates a generalized stress response *via* transcriptional regulation. Comparison of the expression levels of *P5CS1* and *DREB2A* in untreated and salt-treated WT, *gi-1* and GI-OX plants by qRT-PCR analyses showed that salt stress induced expression of these genes in all these lines, albeit with different kinetics and ZT maxima (Fig. 2c,d). In addition, we observed higher induction of DREB2A genes in *gi-1* compared to WT, suggesting GI acts as a negative regulator of salt- induced DREB2A response even though the response of *P5CS1* was not affected in the *gi-1* mutant. *P5CS1* and *DREB2A* transcript levels were dramatically changed in *sos1-1*, as has been shown previously[31] (Supplementary Fig. S8). Nonetheless the induction of the DREB2A stress response gene was enhanced in *gi-1*, this failed to explain the strong salt tolerance of *gi-1* (Fig. 2a). Together with the fact that salinity controls GI at the posttranslational level (Fig. 1d, e), GI might affect the *Arabidopsis* growth response to salt by a mechanism involving transcriptional reprogramming of stress response genes and also through posttranslational control.

Maintaining ion homeostasis under salt stress is another means for cells to survive. The plasma membrane Na^+/H^+ antiporter SOS1 is a critical determinant of salt tolerance in *Arabidopsis*[31]. The Na^+/H^+ exchanger activity of SOS1 is essential for Na^+ efflux from *Arabidopsis* cells. To ascertain whether *GI* affects SOS1 function, we measured the Na^+/ H^+-exchange activity in purified plasma membrane vesicles from WT, *gi-1* and *sos1-1* plants. When compared with WT, Na^+/H^+-exchange activity was greatly reduced

in vesicles of the salt-sensitive *sos1-1* mutant, and was significantly higher in the salt-tolerant *gi-1* mutant (Fig. 2e). Thus GI appears to act as a negative regulator of salt tolerance by inhibiting Na^+/H^+ exchanger activity of SOS1.

To test whether SOS1 protein levels are affected by GI, we developed an anti-SOS1 antiserum that, albeit it was not completely SOS1-specific, it fails to recognize a protein corresponding to the predicted size of SOS1 (127 kDa) in extracts of *sos1-1* plants (Supplementary Fig. S4). This band is detected in WT and is more abundant in SOS1-OX plants. Using this antibody to estimate SOS1 protein levels, we observed that the *gi-1* mutant accumulated SOS1 protein upon salt stress to a much higher level compared to WT without any evidence of an accompanying increase in SOS1 transcript level (Fig. 2f). The SOS1 over-expressing *gi-1* (SOS1-OX *gi-1*) plants not only accumulated even higher amounts of SOS1 protein than *gi-1* plants, but also exhibited more pronounced tolerance to salt than WT, SOS1OX or *gi-1* plants (Figs 2f, 6a,b). The salt tolerance of the *gi-1* mutant compared to WT can thus be attributed to enhanced plasma membrane Na^+/H^+-exchange activity due to the elevated level of SOS1 protein in the *gi* line (Fig. 2e). This conclusion is supported by studies in yeast mutants unable to excrete Na^+ that have clearly established the Na^+/H^+ antiporter activity of SOS1[7,9], and by the observation that active SOS1 protein is a requirement for salt tolerance in *Arabidopsis*[32].

GI interacts with SOS2. GI is a partner in protein-protein interactions that affect functions of other proteins[25,33,34]. This led us to reason that GI may influence SOS1 function through direct or indirect protein interaction. To explore the interaction of GI with components of the SOS pathway in plants, we performed co-immunoprecipitation

(co-IP) assays in leaf protein extracts from tobacco plants that were transiently expressing GI-HA with SOS1-GFP, SOS2-GFP, or SOS3-myc fusions. The results showed that GI interacts with SOS2 and SOS3, possibly in a complex preformed *in planta*, whereas GI did not significantly interact with SOS1 (Fig. 3a). Since SOS2 and SOS3 are known to interact *in planta*[8,9], further tests determined whether one or both proteins interacted directly with GI. A pull-down assay using combinations of *in vitro* translated ^{35}S-labeled GI protein and GST-SOS3, GST-SOS2 or GST (negative control) established that GI interacted strongly with SOS2 but not with SOS3 or GST (Fig. 3b). The interaction of GI with SOS2 but not SOS3 was confirmed using a yeast split-ubiquitin assay based on the reassembly of ubiquitin (Ub) due to interaction of the fusion partners of its N- and C- terminal fragments (Nub and Cub). Only cells co-expressing Nub-SOS2 and GI-Cub-RUra3p were unable to grow on plates without uracil, but grew on plates containing 5-fluoroorotic acid (FOA), indicating that only SOS2 formed stable complexes with GI (Fig. 3c). Thus, GI interacts with SOS2 directly *in vivo* and *in vitro*.

This result suggested several possibilities for the function of GI as a negative regulator of salt tolerance. Since the calcium-dependent SOS2-SOS3 protein complex activates SOS1, GI could either interfere with the SOS2-dependent up-regulation of SOS1 or it could mask or disperse the influence of the sodium-sensing Ca^{2+}-binding protein SOS3 (CBL4) on SOS2. It appeared also possible that the GI-SOS2 complex might have a specific function in the plant nucleus by which the transition to flowering is

accelerated. In the latter, highly hypothetical scenario, GI would direct the normally cytosolically localized protein kinase SOS2 into the nucleus.

GI inhibits SOS2-mediated SOS1 phosphorylation. SOS2 encodes a serine/threonine protein kinase of the SNF1/AMPK family that activates the Na^+/H^+ antiporter SOS1 through phosphorylation of SOS1 at its C-terminus (amino acids 441-1146)[7]. To determine whether GI-SOS2 interaction affects phosphorylation of SOS1 by SOS2, an *in vitro* kinase assay was performed using a mutant SOS2 kinase (GST-$SOS2^{T168D}$)[35,36], that is more active than native SOS2 and is independent of SOS3. A C-terminal fragment of SOS1 was used as substrate. Inclusion of purified recombinant GI in the kinase reaction greatly reduced the phosphorylation level of SOS1 whereas the inclusion of BSA had no significant effect (Fig. 4a) leading to the conclusion that GI binds to SOS2 and renders it unavailable for SOS1 phosphorylation. The result was confirmed by demonstrating phosphorylation of SOS1 *in vivo*. SOS2-dependent phosphorylation of SOS1 *in planta* can be demonstrated in salt stressed plants using anti-SOS1 antibody. Phosphorylated SOS1 is detected on immunoblots as a mobility-retarded band[7]. We detected significant amounts of the mobility-retarded, phosphorylated SOS1 band in the *gi-1* and *gi-201* plants compared to WT and SOS1-OX plants (Fig. 4b). Taken together, the *in vitro* and *in vivo* results revealed a negative effect of GI on SOS2-dependent phosphorylation of SOS1.

SOS1 phosporylation status is critical for SOS1 stability. We next tested whether SOS1 stability was affected by its salt-induced phosphorylation status. A cell-free degradation assay was used consisting of the incubation of total protein extracts

from salt-treated *35S::SOS1-HA* plants with or without phosphatase. The relative degradation rate of HA-tagged SOS1 was measured by western blot analysis using anti-HA antibody. SOS1 protein levels declined more rapidly after phosphatase treatment indicating that the dephosphorylated SOS1 was more labile than its phosphorylated form (Fig. 5a,b). This strongly suggested that salt stress-induced phosphorylation of SOS1 could have a role in stabilizing the protein.

A functional SOS2 is required for phosphorylation of SOS1 upon salt stress[7]. Studies in *Saccharomyces cerevisiae* have established that two specific serine residues of SOS1, S1136 and S1138, are essential and sufficient for activation by SOS2 and re-establishment of cellular ion homeostasis[7]. The role of SOS2-dependent phosphorylation in SOS1 stabilization *in vivo* was therefore verified by comparing SOS1 protein levels in NaCl-treated leaves of WT, *sos1-1*, SOS1-OX-DAPA (*35S:SOS1*$^{S1136A/S1138A}$) and SOS1-OX plants. Indeed, NaCl-induced accumulation of SOS1 protein was observed in SOS1-OX but not in SOS1-OX-DAPA plants although the *SOS1* transcript levels were comparable in these two lines (Fig. 5c). On the basis of this result, we hypothesized that GI prevents SOS1 phosphorylation by inhibiting SOS2 kinase activity. This predicates that the salt tolerance phenotype caused by the inactivation of *GI* should be SOS2-dependent. We generated the double mutant, *sos2-2 gi-1,* and conducted tests for salt tolerance in soil with 5 weeks old plants. Indeed, *sos2-2 gi-1* double mutant plants did not exhibit the salt tolerance of single *gi* mutants (Fig. 5d and Fig. 6a,d). Similarly, *gi*-dependent salt tolerance was suppressed in the *sos1-1 gi-1* and also in the null *sos3-1 gi-1* mutant that is impaired in SOS2-dependent

phosphorylation of SOS1 (Fig. 6a,c,e). The steady-state levels of SOS1 protein in the salt-stressed *gi-1* mutant was higher than that in identically treated WT, *sos2-2* and *sos2-2 gi-1* plants, as expected if the effect of GI on the SOS1 level *in planta* is mediated via SOS2 (Fig. 5e). Thus it appears that inhibition of the SOS2-dependent phosphorylation and stabilization of SOS1 is the basis of the negative regulatory role of GI in the SOS pathway.

Salt and SOS3 affect the interaction between GI and SOS2. GI degrades as a result of salt treatment (Fig. 1d). To test whether its interaction partner, SOS2, is necessary for GI degradation, diurnal oscillation of GI level was examined in WT and *sos2-2* plants expressing the *GI:GI-HA* transgene after treatment with 0 or 100 mM NaCl at ZT0 (Supplementary Fig. S5). The *GI:GI-HA* plants express native level of HA-tagged GI[33]. In absence of salt, GI-HA protein oscillated strongly in both WT and *sos2-2*, even though the overall level of GI was lower in *sos2-2* than in WT. The fraction of GI degraded upon salt treatment was comparable in *sos2-2* and WT. This suggests that SOS2 has no significant effect on salt-dependent GI degradation.

We then investigated the effects of NaCl treatment on the steady state level of the GI-SOS2 complex *in vivo*. Tobacco plants transiently expressing combinations of GI-HA and SOS2-GFP were treated or not with NaCl and protein extracts were subjected to co-immunoprecipitation analyses. Compared with untreated controls, the amount of GI found in the GI-SOS2 protein complex pulled down with anti-GFP antibody was

significantly lower after NaCl treatment (Fig. 7a). Re-establishment of cellular ion homeostasis under salt stress is initiated by binding of the calcium sensor SOS3 to SOS2[37] raising the possibility that SOS3 can compete with GI for binding to SOS2. Co-immunoprecipitation assays performed as above revealed that the SOS2-GI interaction *in planta* was indeed abolished by over-expression of SOS3 (Fig. 7a).

SOS3 physically interacts with the protein kinase SOS2 *via* the SOS2 C-terminal regulatory domain that then abolishes auto-inhibition of phosphorylation of SOS2[38]. To test the nature of the competitive relationship between GI and SOS3, we examined whether this competition was centered on the SOS2 regulatory domain. Compared to full length SOS2, the C-terminally truncated SOS2 protein (SOS2-N) showed reduced binding of GI in a pull-down assay with *in vitro* radiolabeled GI (Fig. 7b). Yeast two-hybrid experiments demonstrated that the C-terminal domain SOS2 (SOS2-C) interacts with GI (Fig.7c). Bimolecular fluorescence complementation (BiFC) experiments in tobacco confirmed that C-terminal truncation of SOS2 abolished SOS2-GI interaction and also demonstrated that specific interaction of GI with SOS2 occurs both in the cytosol and nucleus (Fig. 7d). The observation that SOS3 and GI bind to the same domain of SOS2 explains the competition between SOS3 and GI for interaction with SOS2.

Discussion

Here we identify GI, originally described as a gene regulating flowering time, as a major component of the salt stress adaptation pathway. The data fit into a model (Fig. 8) of a novel, unexpected function for GI as a regulator of the salt stress response. This role of GI combined with its known role in flowering allows coordination of flowering time with the salinity stress status of the juvenile plant. According to the model, the crucial salinity defense module is the dynamic protein complex consisting of GI and SOS2 kinase, the activator of the Na^+/H^+ antiporter SOS1. Although GI is predominantly nuclear localized, it is known to be constitutively present at low levels in the cytosol in all tissues[33]. Accordingly, the model (Fig. 8) shows GI binding with SOS2 in the cytosol to inhibit the SOS2-dependent phosphorylation of SOS1. In the absence of salt stress, GI binds to and inhibits the SOS2 function, keeping the SOS system in a resting state. Upon salt stress, GI undergoes proteasomal degradation, releasing SOS2 for interaction with SOS3. This promotes generation of the SOS2-SOS3 complex that activates SOS1 to re-establish ion homeostasis[7,9]. A consequence of the NaCl stress-dependent degradation of GI protein is the frequently observed delay in the initiation of flowering, which connected both processes. The GI-SOS2 complex was also observed in the nucleus (Fig. 7d), but there is no evidence that the SOS pathway might control flowering time (Supplementary Fig. S7). However, a role for the nuclear GI-SOS2 complex in controlling salt tolerance cannot be excluded. Hypothetically, this may explain the exceptional salt tolerance associated with the inactivation of *gi*.

GI has traditionally been associated with the promotion of flowering in long day growth[25,24,27,28]. The genetic and biochemical mechanisms by which GI promotes flowering in long days are well-studied. GI was first identified in a screen for flowering time mutants in *Arabidopsis*. Since then deficiencies in GI have been shown to affect seedling photomorphogenesis in continuous red light[22]. *gi* lines affect the circadian clock and flowering time through controlling the stability of F-box proteins and transcription factor turnover. *gi* mutants show excessive starch accumulation, altered sucrose metabolism and enhanced sensitivity to light and oxidative stress[39,40]. Nonetheless, a molecular basis for the function of this protein has remained elusive as there are no known homologues outside plants, and there is no clear domain structure that might give clues to its function. Molecular interactors for GI, in the form of F-box proteins, have so far been identified in the context of the circadian clock and flowering. Another notable GI-interacting protein is SPINDLY, an O-linked N-acetylglucosamine transferase that negatively regulates flowering time and responses to growth-promoting gibberellins. SPINDLY appears to stabilize DELLA proteins, negative regulators of gibberellin (GA) signaling, in an unknown way[41,42]. *Arabidopsis* plants lacking four *DELLA* genes are salt-sensitive whereas stabilized DELLA proteins enhance salt tolerance, but the precise connection between GI and DELLA-mediated salt tolerance, if any, remains unknown[4,5,6]. Our results, provide a clear molecular connection between the circadian clock, metabolism and salinity stress tolerance. In our model (Fig. 8), GI conditionally interacts with the SOS2 protein kinase in the cytoplasm. This protein complex of conditional stability identifies the missing link between flowering and the specific

adaptation to salt stress conditions. When our results are considered along with earlier reports[4,5,6,41,42], it would appear that GI plays a focal role from which other regulatory processes emerge to control vegetative growth rate, flowering time and stress tolerance. Through protein-protein interactions GI can be considered to act as a switch, partitioning and thus controlling diverse signaling intermediaries. Stability of GI would, in turn, determine the output of these pathways by sequestering or releasing interacting partners.

The trigger that initiates flowering is connected to components of the circadian clock and regulated by the photoperiod to a large degree. Engrained circadian rhythmicity affects transcription of a large number of genes. In addition, multiple stress response pathways are influenced by the circadian rhythm and flowering, with cold responses and vernalization constituting well-studied examples[13,43,44]. GI regulates circadian rhythms by mediating light input to the clock. Transcript levels of the salt-induced *RD29A (COR78)* gene are known to oscillate with a peak at ZT8-10 in basal media[45,46]. We show that the salt-induced expression of *RD29A* is in fact gated by the clock and that the clock affects RD29A gene expression (Supplementary Fig. S6).

Of the genes known to be under circadian control 68% encode stress responsive functions[45]. Arguably, a possibly important function of the clock could be to anticipate and also integrate emerging stress conditions.

The recognition of the interaction between vegetative growth, flowering and salinity tolerance provided here should influence strategies for the creation of salt tolerant plants. The level of salt tolerance attained through the loss of GI is exceptional,

exceeding the effect observed by the over-expression of SOS1 in *Arabidopsis*[47]. This could suggest that the role of GI in recruiting abiotic stress protection may extend beyond its effect on SOS2. Our results can be expected to initiate entirely new research directions in the understanding and manipulation of salt tolerance in crop plants.

Methods

Plant materials and salt stress treatments. *Arabidopsis thaliana* mutants and transgenic lines *sos1-1, sos2-2, sos3-1,* SOS1-OX, SOS1HA-OX *gi-1, gi-2, gi-201,* GIHA-OX, and GI:GI-HA were in Columbia (*Col-0*) background[29,33,38]. Lines *gi-1 sos1-1, gi-1 sos2-2, gi-1 sos3-1, gi-1* SOS1-OX and *sos2-2* GI:GI-HA were generated by genetic crossing. Genotypes were verified by PCR and flowering times were recorded. Unless otherwise specified, plants were grown at 23°C (16 h light / 8 h dark). To examine flowering time (Figs. 1a,b; Supplementary Figs. S1, S7), seeds were germinated and grown on basal medium [½ Murashige and Skoog (MS) salts, 2 % sucrose] solidified with 1 % agar, without or with NaCl supplement, in growth bottles (500 ml; 14 cm in height; five plants per bottle) with good air exchange. Flowering time was measured either by counting numbers of leaves (rosette + cauline) when bolted stems were ~1 cm long, or as days to bolting. For testing salt-tolerant phenotypes (Figs. 2a and 5d), seeds were germinated in basal medium and 10 day-old seedlings were transferred to soil. Seventeen-day-old plants on soil were watered with indicated concentrations of NaCl twice per week for 2 weeks. For immunoblot analysis (Figs. 1d, 2f, 4b, and 5c,e), leaves detached from 3-week-old soil-grown plants were treated with

NaCl at ZT1 (Zeitgeber Time 1) and harvested at times indicated in the legends. For salt treatment of seedlings, two-week-old seedlings grown on filter paper (Advantec) in basal medium were treated with 100 mM NaCl at ZT0 by flooding the filter paper on salt solutions and harvested at times indicated (Figs 2c,d, 6; Supplementary Figs. S3, S6). NaCl treatment was restricted to ZT0-ZT4 since plants were most responsive to stress during this interval, as established by measuring NaCl-induction of *RD29A* transcript levels (Supplementary Fig. S6). RD29A has been characterized as a strongly salinity up-regulated transcript[48].

Plasma membrane isolation and Na^+/H^+ antiport assays. Vesicles were isolated from 5-week-old plants by two-phase partitioning[49]. Na^+/H^+ antiport activity was measured at 30°C as Na^+-induced dissipation of the pH gradient established by the activity of the plasma membrane H^+-ATPase in inside-out plasma membrane vesicles isolated from leaves of WT, *gi-1* and *sos1-1* plants. Changes in pH during the assay were monitored as quenching of the pH-sensitive fluorescent probe 9-amino-6-chloro-2-methoxyacridine (ACMA)[50]. Assays (1 ml) contained 20 µg of plasma membrane protein, 1 µM ACMA, 50 mM 1,3-bis[tris(hydroxylmethyl) methylamino]propane (BTP)-HEPES (pH 7.5), 3 mM ATP-BTP (pH 7.5), 250 mM mannitol, 50 mM KNO_3, and 0.075% Brij58. Reactions were equilibrated in the dark with stirring for 5 min before beginning monitoring. Assays were initiated by the addition of 3 mM $MgSO_4$. After reaching steady state baseline fluorescence, Na^+ transport was initiated by adding NaCl. The initial rate of dissipation ($\Delta F\ min^{-1}$) was measured by changes in fluorescence during the first 10 s after addition of Na^+. Reactions were terminated by adding 10 mM

(final concentration) of $(NH_4)_2SO_4$ to dissipate any remaining ΔpH and obtain the maximum fluorescence (Fmax). Fluorescence was recorded in a fluorescence spectrophotometer with a thermostated, stirred cell (Hitachi model FL-2500) at excitation and emission wavelengths of 415 and 485 nm, respectively. Activities are expressed in arbitrary units as the relative change in fluorescence (ΔF/Fmax) min^{-1} mg^{-1} membrane protein).

RNA isolation and expression analysis. Total RNA was extracted using RNeasy Plant Mini Kit (Qiagen) and treated with DNase (Sigma). First-strand cDNA was synthesized using the Thermoscript^{TM} RT-PCR System (Invitrogen). PCR amplification used e-Taq DNA polymerase (Solgent). Gene-specific primers are listed in Supplementary Table S1. RT-PCR conditions were as follows: 94°C for 2 min, 25 (for *GI*) or 30 (for *SOS1*) cycles of 94°C for 30 s, 54°C for 30 s, and 72°C for 1 min, followed by 72°C for 5 min. Conditions for *CO, FT, P5CS1* and *DREB2A*) were 95°C for 5 min, 45 cycles of 95°C for 10 s and 60°C for 30 s, followed by 95°C for 10 s, 65°C for 5 s, and 95°C for 5 s. Amplified products were detected using Power SYBR Green PCR master mix (Applied Biosystems) in a Bio-Rad C1000TM Thermal Cycler. The efficiency value of amplification for each primer set was checked by measuring the abundance of transcripts from cDNA dilutions according to the manufacture guide book (Real-Time PCR applications guide, Bio-Rad). Each data point shown is the average of two independent amplifications of the same RNA sample run in the same reaction plate. At least two independent RNA samples for each genotype and condition were used.

Cloning. For details see Supplementary Methods.

Preparation of Recombinant Proteins. For details see Supplementary Methods.

***In vitro* Binding Assays**. ^{35}S-Met labeled GI protein was generated using *in vitro* transcription/translation (TNT Quick Coupled Transcription/Translation System, Promega). ^{35}S-Met labeled proteins were incubated with equal amounts of GST, GST-SOS2 proteins, or GST-SOS3 and glutathione-cellulose beads for 1 h at 4°C in 100 µl of binding buffer (20 mM Tris-HCl, pH 7.5, 100 mM KCl, 50 mM NaCl, 0.5% NP-40, 10% glycerol, 5 µg ml^{-1} BSA, 1% Triton X-100, 1 mM PMSF, 5 µg ml^{-1} leupeptin, 5 µg ml^{-1} aprotinin, 1 µg ml^{-1} pepstatin, 5 µg ml^{-1} chymostatin, 5 µg ml^{-1} antipain, 50 µM MG132, 1 mM DTT, and phosphatase inhibitors (1 mM each of NaF and Na_3VO_4). Beads were washed and re-suspended in 15 µl of 2X SDS sample buffer. Proteins released were separated by 10% SDS-PAGE, gels vacuum-dried, and radiolabeled proteins detected by Cyclone (Perkin Elmer).

Kinase Assay. Kinase reactions were set up essentially as described[51,52]. Combinations of purified bacterially expressed GST-SOS1 CD3 (substrate), GST-SOS2^{T168D}, MBP-GIN(1-391) and BSA were incubated with 0.6 µl of [γ-^{32}P] ATP (6 µCi) in kinase buffer (20 mM Tris-HCl, pH 7.5, 10 mM $MgCl_2$, 0.5 mM $CaCl_2$, 2 mM DTT) at room temperature for 1 h followed by the addition of 6X SDS loading buffer. Separated by 8% SDS-PAGE, protein gels were stained, de-stained and dried and radiolabeled proteins visualized using a Cyclone phosphor-imager (Perkin Elmer)[35,36].

Bimolecular Fluorescence Complementation assays. *Agrobacterium tumefaciens* strain GV 3101 transformed with test constructs was grown in LB medium supplemented with 10 mM MES, 20 μM acetosyringone, and antibiotics appropriate for particular constructs. Cells were collected by centrifugation and washed twice with infiltration solution (10 mM $MgCl_2$, 10 mM MES, and 100 μM acetosyringone). *Agrobacterium* cultures including cells harboring p19 silencing plasmid was adjusted to OD_{600}=0.5 in infiltration solution. Leaves of 4-week-old *Nicotiana benthamiana* plants were co-infiltrated with the desired combination of cultures and the plants were incubated for 2 days. Fluorescence of reconstituted YFP was detected using a confocal laser scanning microscope (Olympus FV1000) at excitation wavelength 515 nm.

Immunoblot Analysis and Immunoprecipitation. Protein was extracted in 100 mM Tris-Cl, pH 7.5, 150 mM NaCl, 0.5% NP-40, 1 mM EDTA, 3 mM DTT and protease inhibitors (1 mM PMSF, 5 μg ml^{-1} leupeptin, 1 μg ml^{-1} aprotinin, 1 μg ml^{-1} pepstatin, 5 μg ml^{-1} antipain, 5 μg ml^{-1} chymostatin, 2 mM Na_2VO_3, 2 mM NaF and 50 μM MG132) and separated on SDS-PAGE[33]. For analysis of SOS1 levels after phosphatase treatment, extracts were prepared either in 1X phosphatase buffer supplemented with 2.5 mM $MnCl_2$, 0.5% Triton X-100, and 0.4% Nonidet P-40, or in New England Biolabs (NEB) Buffer 3 with 5 μg ml^{-1} antipain, 5 μg ml^{-1} chymostatin, 1 μg ml^{-1} pepstatin, 5 μg ml^{-1} leupeptin, 5 μg ml^{-1} aprotinin, 1 mM PMSF, 50 μM MG132, 50 μM MG115, and 50 μM ALLN (Acetyl-L-Leucyl-L-Leucyl-L-Norleucinal). Aliquots (50 μl) of protein extracts were incubated with 400 units of lambda protein phosphatase (NEB) at 30°C for 5 min in the absence or presence of phosphatase inhibitors (2 mM NaF, 2 mM Na_3VO_4).

Immunoblot analysis was carried out using rat α-HA (1:2000; Roche) for SOS1-HA and GI-HA detection or mouse α-SOS1 (1:250) antibody. The antigen protein was detected by chemiluminescence using an ECL-detecting reagent (Thermo Scientific).

Immunoprecipitation for interactions between GI and SOS proteins. GI-HA and SOS1-GFP, SOS2-GFP, or SOS3-MYC were transiently expressed in *N. benthamiana* leaf cells by *Agrobacterium* infiltration. For immunoprecipitation, rabbit anti-GFP polyclonal (1:250; Abcam) or mouse anti-MYC monoclonal (1:250; Cell Signaling Technology) antibodies were pre-incubated with protein A agarose (Invitrogen) at 4°C. Then protein extracts (GI-HA and SOS1-GFP, GI-HA and SOS2-GFP, GI-HA and SOS3-MYC) were added and incubation continued for 1 h. Complexes were separated by SDS-PAGE and immunoblotted as described previously[33]. Each immunoblot was incubated with the appropriate primary antibody (anti-HA antibody, 1:2000; anti-GFP antibody, 1:5000; anti-MYC antibody, 1:1000) for 4 h at room temperature or overnight at 4°C. Membranes were developed using peroxidase-conjugated secondary antibody (1:1000-3000) [anti-rat IgG (Sigma), anti-mouse IgG (Santa Cruz Biotechnology), and anti-rabbit antibody (GE Healthcare)], and proteins were detected by ECL as described above.

Yeast Split-Ubiquitin Assay. For split-ubiquitination assays[53] plasmids were transformed into *S. cerevisiae* strain JD53 using PEG and heat shock (Clontech protocol). Interactions between pairs of proteins were tested on selective medium containing 1.5 mg ml^{-1} 5-FOA (5-Fluoroorotic acid monohydrate; Zymo Research) and

selective medium lacking uracil. Plates were photographed after incubation at 30°C for 3-5 days. Assays were each performed twice, and each experiment included three biological replicates.

Interaction between GI and SOS2. For yeast two-hybrid assays, constructs were transformed into yeast strain HF7c. Growth of transformants was monitored on synthetic complete medium lacking Trp, Leu, +/- His. Three independent transformants of each *SOS2* construct were tested for interaction with *GI*. Empty *pACT2* provided the negative control.

Author contributions list

W.Y.K., Z.A., and H.J.P. contributed equally to the work as first authors. W.Y.K., Z.A., and D.J.Y. initiated the project and W.Y.K., S.Y.L, H.J.B., J.M.P., and D.J.Y. analyzed the data. W.Y.K., Z.A., H.J.P., S.J.P., J.Y.C., J.P.H., F.J.Q., G.S., M.R.K., Z.Q., L.N., and H.C.P performed the experiments. W.Y.K., R.A.B., H.J.B., and D.J.Y. wrote the paper with input from other authors. All authors discussed the results and approved the manuscript.

ACKNOWLEDGEMENTS. This research was supported by the Next-Generation BioGreen 21 Program (Systems and Synthetic Agrobiotech Center, no. PJ008025), a

Cooperative Research Program for Agriculture Science & Technology Development (Project No. PJ007850), and the Ministry of Education, Science and Technology for the World Class University (WCU) program (R32-10148) from the Rural Development Administration, Republic of Korea, and by grant BIO2009-08641 financed by the Spanish Ministry of Science and Innovation and the FEDER program.

FIGURE LEGENDS

Figure 1. GI regulates the initiation of flowering in response to salt stress.

(a and b) Salt treatments delay flowering in *Arabidopsis*. WT (Col-0), *gi-1,* and GI-OX (*35S::GI-HA*) plants were grown under long-day conditions (16 h light/8 h dark) on MS media without and with 50 mM (a) or 25 mM NaCl (b) supplement. Plants were photographed at 5 weeks. Mean (± SE) flowering times are shown as number of leaves at bolting. (c) Effect of salt treatment on expression pattern of the flowering time regulator genes *CO* and *FT*. Twenty four hours NaCl treatment (0 and 50 mM) of ten-day-old seedlings grown on MS media was initiated at ZT0 (Zeitgeber Time 0). Transcript levels, normalized to the transcript level of *Actin* (*ACT*), were measured by real time qRT-PCR. Data are the mean ± SE from three biological replicates. (d) GI is degraded upon exposure to salt in a proteasome-dependent manner. Detached leaves of soil-grown 3-week-old GI-OX plants were treated with NaCl (100 mM), MG132 (100 μM) or NaCl plus MG132 at ZT1. GI protein level (GI-HA, left panel) was evaluated after 0 h, 12 h and 24 h treatments by immunoblot analysis with anti-HA antibody. Coomassie brilliant blue (CBB)-stained blots are shown as loading control. Molecular weight markers in kDa. *GI* and *Tubulin* (*TUB*, internal control) transcript levels (right panel) were evaluated by RT-PCR. All experiments were repeated at least three times. (e) Quantification of the results shown in (d, left panel). Relative GI protein (fold) is the ratio of the GI signal at a given time to the GI signal at ZT0. Values represent mean ± SE (n=3).

Figure 2. Salt tolerance in the *gi* mutant is mediated by increased Na^+/H^+ exchange activity.

(a and b) The *gi* mutant exhibits increased salt tolerance. (a) WT, *gi-1,* and GI-OX plants were grown on soil for 3 weeks (top panel) and then treated with 0 mM (middle) or 150 mM (bottom) NaCl for 2 weeks. Plants are shown (a) representative of ten to twelve individual plants that were examined for each line. (b) Fresh weight at the end of the treatments shown in (a). Index indicates the percent decrease in average fresh weight after NaCl treatment. Data represent the mean ± SE of the three independent replicates. (c and d) qRT-PCR analysis of *P5CS1* (c) and *DREB2A* (d) transcript levels over 20 h NaCl treatment. Ten-day-old seedlings were treated with (dotted line) or without (solid line) 100 mM NaCl at ZT0. *TUBULIN2 (TUB2*) was used as internal control. Data represent the mean ± SE of three independent experiments. White-and-black bar represents light and dark periods, respectively. (e) Na^+/H^+ exchange activity in plasma membrane vesicles isolated from WT, *gi-1*, Col-0, and *sos1-1* leaves is shown as a function of Na^+ concentration in the assay medium. Each point is the average of three technical replicates ± SD. (f) SOS1 abundance increased in the *gi* mutant. Leaves of 3-week-old WT, SOS1-OX, *gi-1,* and SOS1-OX x *gi-1* plants were treated with 100 mM NaCl for 24 h. SOS1 was detected in total protein extracts by immunoblotting with anti-SOS1 antibody. Molecular weight markers in kDa. The CBB-stained membrane is shown as a loading control. The bottom two panels represent RT-PCR analysis of the *SOS1* and *TUBULIN2* (*TUB,* control) transcript levels in these leaves. All experiments were repeated at least three times.

Figure 3. GI directly interacts with SOS2.

(a) GI interacts with SOS2 and SOS3 *in vivo*. Tobacco plants were infiltrated with *Agrobacterium* harboring *35S::GI-HA* and *35S::SOS1-GFP*, *35S::SOS2-GFP* or *35S::SOS3-MYC* for transient expression. Protein extracts (Input) were immunoprecipitated (IPed) with anti-GFP or anti-MYC antibodies and resolved by SDS-PAGE. The shown immunoblots were developed with anti-HA to detect GI, anti-GFP to detect SOS1 or SOS2, and anti-MYC to detect SOS3 (b) GI interacts with SOS2 *in vitro*. Shown is the autoradiograph (top panel in b) and CBB stain (bottom in b) of a gel containing resolved affinity-purified binding reactions that contained ^{35}S-GI, GST (negative control), GST-SOS2 and GST-SOS3 proteins in indicated combinations. Molecular weight markers in kDa. (c) GI interacts with SOS2 in the yeast split-ubiquitination assay. Positive and negative controls (C) represent yeast cells harboring the *pMet-SIZ1-Cub* + *pCup-NuI-SUMO1* and *pMet-Cub* + *pCup-NuI* vectors, respectively. GI was fused to the N-terminus and either SOS2 or SOS3 were fused to the C-terminus of ubiquitin.

Figure 4. GI inhibits SOS2-mediated SOS1 phosphorylation.

(a) GI inhibits SOS2-mediated SOS1 phosphorylation *in vitro.* An *in vitro* kinase assay was performed including purified bacterially GST-SOS1 CD3 (SOS1 C-terminus, amino acids 885 to 1146), GST- SOS2^{T168D}, MBP-GIN (GI N-terminus, amino acids, 1-

391) and BSA (negative control) proteins in the indicated combinations. Shown are the autoradiogram (top panel) and CBB stain (middle) of a gel containing resolved reactions, and quantification of the SOS1 signals (n= 3 ± SD; bottom panel). (b) Phosphorylated SOS1 protein accumulates in salt-stressed *gi* plants. Leaves of three-week-old soil-grown *sos1-1,* WT, SOS1-OX, *gi-1,* and *gi-201* plants were treated with 100 mM NaCl for 24 h. Immunoblot analysis of total protein extracts was performed with anti-SOS1 using CBB-stained bands as loading control. Molecular weight markers in kDa.

Figure 5. SOS2-dependent phosphorylation is critical for SOS1 protein stability and is increased in the *gi* mutant.

(a and b) Dephosphorylation of SOS1 increases its rate of degradation in cell extracts. Protein extracts of NaCl-treated (100 mM, 24 h) SOS1HA-OX plants were incubated with lambda phosphatase at 30°C for the indicated time periods in the presence (Control) or absence (Phosphatase) of phosphatase inhibitors and then subjected to immunoblot analysis with anti-HA antibody (upper panel). The CBB-stained bands are shown as loading control (lower panel). (b) Quantification of SOS1 protein levels shown in (a). Data represent mean ± SE of three independent experiments. (c) SOS2-dependent phosphorylation is critical for SOS1 protein stability. Total protein extracts from NaCl-treated (100 mM, 24 h) leaves of three week-old WT, *sos1-1,* SOS1-OX-DAPA (overexpressing SOS1 mutated at the SOS2-target phosphorylation sites[7]),

and SOS1-OX plants were subjected to immunoblot analysis with anti-SOS1 antibody. The CBB-stained bands provide a loading control. The *SOS1* transcript level was confirmed by RT-PCR. *TUBULIN2* (*TUB*) transcripts (bottom row) provide a loading control. (d) SOS2 is required for *gi-1*-mediated salt tolerance. Shown are WT, *sos2-2*, *gi-1,* and *sos2-2* x *gi-1* double mutant plants that were grown in long day conditions (16 h light/8 h dark) on soil for 3 weeks (Before) and then (After) watered with 0 mM (middle row) or 150 mM (bottom row) NaCl solution for two weeks. (e) SOS2 is necessary for accumulation of SOS1 in *gi-1*. Protein extracts of *sos2-2, gi-1, sos2-2* x *gi-1* double mutant, and WT plants treated with 100 mM NaCl for 24 h were subjected to immunoblot analysis as in (c). (a, c and e) Molecular weight markers in kDa.

Figure 6. GI is involved in salt-sensitive signal transduction.

(a) Seeds from indicated lines were grown on basal medium without (0 mM) or with 50 mM NaCl supplement under long-day conditions (16 h light/8 h dark) and photographed after 14 days. (b-e) Plants were grown on soil under the same long day condition for 3 weeks (first row, Before) and then (After) watered with water (0 mM NaCl) for one week (second row), 300 mM NaCl solution for one week (third row) or 300 mM NaCl solution for two weeks (fourth row). Genotypes used: WT, *gi-1*, GI-OX (*35S:GI-HA*), SOS1-OX (*35S:SOS1*), *sos1-1*, *sos2-2*, *sos3-1*, and double mutants SOS1-OX x *gi-1*, *sos1-1* x *gi-1*, *sos2-2* x *gi-1*, *sos3-1* x *gi-1*.

Figure 7. Salt and SOS3 affect the interaction between GI and SOS2.

(a) Salt and SOS3 interfere with GI-SOS2 interaction *in vivo*. *35S::GI-HA, 35S::SOS2-GFP* and *35S::SOS3-MYC* constructs in the indicated combinations were transiently expressed in tobacco leaves by *Agrobacterium* infiltration. Shown are immunoblots of total protein extracts from leaves treated with 0 (-NaCl) or 100 mM NaCl (+NaCl) for 24 h that were fractionated by SDS-PAGE before (Input) or after immunoprecipitation with anti-GFP antibody (IP:αGFP). Blots were developed using tag-specific antibodies. (b) GI interacts with the C-terminus of SOS2. *In vitro*-translated ^{35}S-GI was incubated with GST (I) or the fusion proteins GST-SOS2-F (II; full length SOS2, 1-446 aa) or GST-SOS2-N (III; SOS2 N-terminal catalytic domain, 1–308 aa). After pull-down with glutathione-cellulose, the protein complexes were resolved by SDS-PAGE and detected by autoradiography and CBB staining. (a and b) Molecular weight markers in kDa. (c) GI interacts with the C-terminus of SOS2. Shown are the results of a yeast two-hybrid assay using full-length GI protein (GI) as prey and SOS2-N or SOS2-C (SOS2 C-terminal regulatory domain, 309–446 aa) as bait. Empty vector was used as a negative control prey. Decimal dilutions of three independent cultures co-transformed with GI and SOS2 constructs were plated. Growth without histidine supplementation (-HIS) indicates positive interaction. (d) GI interacts with the C-terminus of SOS2 *in vivo*. Shown are the results of BiFC analyses performed with constructs containing Venus fluorescent protein N-terminal (VN) alone or fused to GI (GI-VN) and constructs containing Venus fluorescent protein C-terminal (VC) alone or fused to SOS2-F (VC-

SOS2) or SOS2-N (VC-SOS2-N). Shown are images of tobacco protoplasts (top row) and epidermal cell layers (rows 2-5) that were isolated from infiltrated leaves.

Figure 8. A model for GI as a negative regulator of salt tolerance.

In the absence of salt stress (-NaCl), GI binds to SOS2 and prevents interaction with the activating protein SOS3. Salt stress (+NaCl) triggers the degradation of GI, releasing SOS2. Free SOS2 then interacts with SOS3 to form an active SOS2-SOS3 protein kinase complex that translocates to the plasma membrane, allowing the SOS2-specific phosphorylation and activation of SOS1 that promotes salt stress tolerance.

References

1. Parida, A. K. & Das, A. B. Salt tolerance and salinity effects on plants: a review. *Ecotoxicol. Environ. Saf.* 60, 324-349 (2005).
2. Yamaguchi-Shinozaki, K. & Shinozaki, K. Transcriptional regulatory networks in cellular responses and tolerance to dehydration and cold stresses. *Annu. Rev. Plant Biol.* 57, 781-803 (2006).
3. Shinozaki, K. & Yamaguchi-Shinozaki, K. Molecular responses to dehydration and low temperature: differences and cross-talk between two stress signaling pathways. *Curr.Opin. Plant Biol.* 3, 217-223 (2000).
4. Achard, P. *et al.* Integration of plant responses to environmentally activated phytohormonal signals. *Science* 311, 91-94 (2006).
5. Maymon, I. *et al.* Cytosolic activity of SPINDLY implies the existence of a DELLA-independent gibberellin-response pathway. *Plant J.* 58, 979-988 (2009).
6. Wasilewska, A. *et al.* An update on abscisic acid signaling in plants and more …. *Mol. Plant* 1, 198-217 (2008).
7. Quintero, F. J. *et al.* Activation of the plasma membrane Na^+/H^+ antiporter Salt-Overly-Sensitive 1 (SOS1) by phosphorylation of an auto-inhibitory C-terminal domain. *Proc. Natl. Acad. Sci. USA* 108, 2611-2616 (2011).
8. Zhu, J.-K. Regulation of ion homeostasis under salt stress. *Curr.Opin. Plant Biol.* 6, 441-445 (2003).
9. Quintero, F. J., Ohta, M., Shi, H., Zhu, J.-K. & Pardo, J. M. Reconstitution in yeast of the *Arabidopsis* SOS signaling pathway for Na^+ homeostasis. *Proc. Natl. Acad. Sci. USA* 99, 9061-9066 (2002).
10. Ausín, I., Alonso-Blanco, C. & Martínez-Zapater, J.-M. Environmental regulation of flowering. *Int. J. Dev. Biol.* 49, 689-705 (2005).
11. Dennis, E. S. & Peacock, W. J. Epigenetic regulation of flowering. *Curr.Opin. Plant Biol.* 10, 520-527 (2007).
12. de Montaigu, A., Téth, R. & Coupland, G. Plant development goes like clockwork. *Trends Genet.* 26, 296-306 (2010).
13. Amasino, R. Seasonal and developmental timing of flowering. *Plant J.* 61, 1001-1013 (2010).
14. Kami, C., Lorrain, S., Hornitschek, P. & Fankhauser, C. Light-regulated plant growth and development. *Plant Development* 91, 29-66 (2010).
15. Srikanth, A. & Schmid, M. Regulation of flowering time: all roads lead to Rome. *Cell Mol. Life Sci.* 68, 2013-2037 (2011).

16. Adams, S. & Carré, I. A. Downstream of the plant circadian clock: output pathways for the control of physiology and development. *Essays Biochem.* 2011, 53-69 (2011).

17. Battey, N. H. & Tooke, F. Molecular control and variation in the floral transition. *Curr.Opin. Plant Biol.* 5, 62-68 (2002).

18. Jablonka, E. & Raz, G. Transgenerational epigenetic inheritance: prevalence, mechanisms, and implications for the study of heredity and evolution. *Q. Rev. Biol.* 84, 131-176 (2009).

19. Lokhande, S. D., Ogawa, K., Tanaka, A. & Hara, T. Effect of temperature on ascorbate peroxidase activity and flowering of *Arabidopsis thaliana* ecotypes under different light conditions. *J. Plant Physiol.* 160, 57-64 (2003).

20. Li, K. *et al.* GA signaling and *CO/FT* regulatory module mediate salt-induced late flowering in *Arabidopsis thaliana*. *Plant Growth Regul.* 53, 195-206-206 (2007).

21. Jung, C. & Müller, A. E. Flowering time control and applications in plant breeding. *Trends Plant Sci.* 14, 563-573 (2009).

22. Oliverio, K. A. *et al.* GIGANTEA regulates phytochrome A-mediated photomorphogenesis independently of its role in the circadian clock. *Plant Physiol.* 144, 495-502 (2007).

23. Suarez-Lopez, P. *et al.* CONSTANS mediates between the circadian clock and the control of flowering in *Arabidopsis*. *Nature* 410, 1116-1120 (2001).

24. Mizoguchi, T. *et al.* Distinct roles of GIGANTEA in promoting flowering and regulating circadian rhythms in *Arabidopsis*. *Plant Cell* 17, 2255-2270 (2005).

25. Sawa, M., Nusinow, D. A., Kay, S. A. & Imaizumi, T. FKF1 and GIGANTEA complex formation is required for day-length measurement in *Arabidopsis*. *Science* 318, 261-265 (2007).

26. Putteril, J., Robson, F., Lee, K., Simon, R. & Coupland, G. The CONSTANS gene of *Arabidopsis* promotes flowering and encodes a protein showing similarities to zinc finger transcription factors. *Cell* 80, 847-857 (1995).

27. Fowler, S. *et al.* GIGANTEA: a circadian clock-controlled gene that regulates photoperiodic flowering in *Arabidopsis* and encodes a protein with several possible membrane-spanning domains. *EMBO J.* 18, 4679-4688 (1999).

28. Park, D. H. *et al.* Control of circadian rhythms and photoperiodic flowering by the *Arabidopsis* GIGANTEA Gene. *Science* 285, 1579-1582 (1999).

29. David, K. M., Armbruster, U., Tama, N. & Putterill, J. *Arabidopsis* GIGANTEA protein is post-transcriptionally regulated by light and dark. *FEBS letters* 580, 1193-1197 (2006).

30. Hayashi, F., Ichino, T., Osanai, M., & Wada, K. Oscillation and regulation of proline content by P5CS and ProDH gene expressions in the light/dark cycles in *Arabidopsis thaliana* L. *Plant Cell Physiol.* 41, 1096-1101(2000).

31. Shi, H., Ishitani, M., Kim, C. & Zhu, J.-K. The *Arabidopsis thaliana* salt tolerance gene SOS1 encodes a putative Na^+/H^+ antiporter. *Proc. Natl. Acad. Sci. USA* 97, 6896-6901 (2000).

32. Qiu, Q.-S., Guo, Y., Dietrich, M. A., Schumaker, K. S. & Zhu, J.-K. Regulation of SOS1, a plasma membrane Na^+/H^+ exchanger in *Arabidopsis thaliana*, by SOS2 and SOS3. *Proc. Natl. Acad. Sci. USA* 99, 8436-8441 (2002).

33. Kim, W.-Y. *et al.* ZEITLUPE is a circadian photoreceptor stabilized by GIGANTEA in blue light. *Nature* 449, 356-360 (2007).

34. Tseng, T.-S., Salomé, P. A., McClung, C. R. & Olszewski, N. E. SPINDLY and GIGANTEA interact and act in *Arabidopsis thaliana* pathways involved in light responses, flowering, and rhythms in cotyledon movements. *Plant Cell* 16, 1550-1563 (2004).

35. Guo, Y. *et al.* Transgenic evaluation of activated mutant alleles of SOS2 reveals a critical requirement for its kinase activity and C-terminal regulatory domain for salt tolerance in *Arabidopsis thaliana*. *Plant Cell* 16, 435-449 (2004).

36. Guo, Y., Halfter, U., Ishitani, M. & Zhu, J.-K. Molecular characterization of functional domains in the protein kinase SOS2 that is required for plant salt tolerance. *Plant Cell* 13, 1383-1400 (2001).

37. Zhu, J.-K. Salt and drought stress signal transduction in plants. *Annu. Rev. Plant Biol.* 53, 247-273 (2002).

38. Halfter, U., Ishitani, M. & Zhu, J.-K. The *Arabidopsis* SOS2 protein kinase physically interacts with and is activated by the calcium-binding protein SOS3. *Proc. Natl. Acad. Sci. USA* 97, 3735-3740 (2000).

39. Kurepa, J., Smalle, J., Van Montagu, M. & Inzé, D. Effects of sucrose supply on growth and paraquat tolerance of the late-flowering *gi-3* mutant. *Plant Growth Regul.* 26, 91-96 (1998).

40. Kurepa, J., Smalle, J., Va, M., Montagu, N. & Inzé, D. Oxidative stress tolerance and longevity in *Arabidopsis*: the late-flowering mutant *gigantea* is tolerant to paraquat. *Plant J.* 14, 759-764 (1998).

41. Silverstone, A. L. *et al.* Functional analysis of SPINDLY in gibberellin signaling in *Arabidopsis*. *Plant Physiol.* 143, 987-1000 (2007).

42. Shimada, A. *et al.* The rice SPINDLY gene functions as a negative regulator of gibberellin signaling by controlling the suppressive function of the DELLA protein, SLR1, and modulating brassinosteroid synthesis. *Plant J.* 48, 390-402 (2006).

43. Kim, D.-H., Doyle, M. R., Sung, S. & Amasino, R. M. Vernalization: winter and the timing of flowering in plants. *Annu. Rev. Cell Dev. Biol.* 25, 277-299 (2009).

44. Covington, M., Maloof, J., Straume, M., Kay, S. & Harmer, S. Global transcriptome analysis reveals circadian regulation of key pathways in plant growth and development. *Genome Biology* 9, R130 (2008).

45. Kreps, J. A. *et al.* Transcriptome changes for *Arabidopsis* in response to salt, osmotic, and cold stress. *Plant Physiol.* 130, 2129-2141 (2002).

46. Dong, M. A., Farré, E. M. & Thomashow, M. F. CIRCADIAN CLOCK-ASSOCIATED 1 and LATE ELONGATED HYPOCOTYL regulate expression of the C-Repeat Binding Factor (CBF) pathway in *Arabidopsis*. *Proc. Natl. Acad. Sci. USA* 108, 7241 -7246 (2011).

47. Shi, H., Lee, B., Wu, S.-J. & Zhu, J.-K. Overexpression of a plasma membrane $Na^{+/}H^{+}$ antiporter gene improves salt tolerance in *Arabidopsis thaliana*. *Nat Biotech* 21, 81-85 (2003).

48. Yamaguchi-Shinozaki, K. & Shinozaki, K. A novel cis-acting element in an *Arabidopsis* gene is involved in responsiveness to drought, low-temperature, or high-salt stress. *Plant Cell* 6, 251-264 (1994).

49. Qiu, Q.-S., Barkla, B. J., Vera-Estrella, R., Zhu, J.-K. & Schumaker, K. S. Na^{+}/H^{+} exchange activity in the plasma membrane of *Arabidopsis. Plant Physiol.* 132, 1041-1052 (2003).

50. Olías, R. *et al.* The plasma membrane Na^{+}/H^{+} antiporter SOS1 is essential for salt tolerance in tomato and affects the partitioning of Na^{+} between plant organs. *Plant, Cell Environ.* 32, 904-916 (2009).

51. Lin, H. *et al.* Phosphorylation of SOS3-LIKE CALCIUM BINDING PROTEIN8 by SOS2 protein kinase stabilizes their protein complex and regulates salt tolerance in *Arabidopsis*. *Plant Cell* 21, 1607-1619 (2009).

52. Fujii, H. & Zhu, J.-K. An autophosphorylation site of the protein kinase SOS2 is important for salt tolerance in *Arabidopsis*. *Mol. Plant* 2, 183-190 (2009).

53. Stagljar, I., Korostensky, C., Johnsson, N. & te Heesen, S. A genetic system based on split-ubiquitin for the analysis of interactions between membrane proteins *in vivo*. *Proc. Natl. Acad. Sci. USA* 95, 5187-5192 (1998).

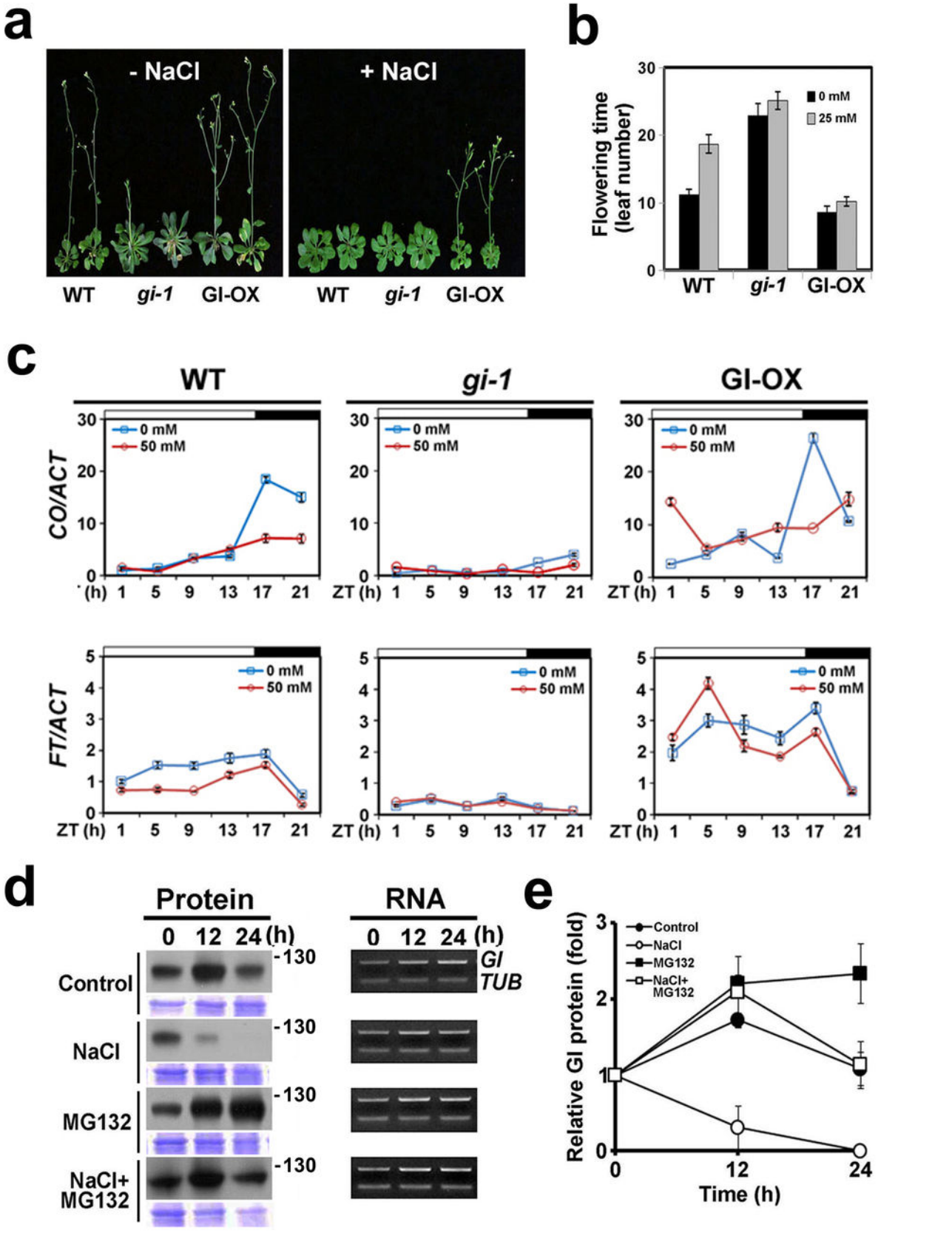
a
- NaCl
+ NaCl
WT
gi-1
GI-OX
WT
gi-1
GI-OX
b
Flowering time (leaf number)
0 mM
25 mM
WT
gi-1
GI-OX
c
WT
gi-1
GI-OX
CO/ACT
FT/ACT
0 mM
50 mM
ZT (h)
d
Protein
RNA
0 12 24 (h)
Control
NaCl
MG132
NaCl+ MG132
-130
GI
TUB
e
Relative GI protein (fold)
Control
NaCl
MG132
NaCl+ MG132
Time (h)

Figure 1

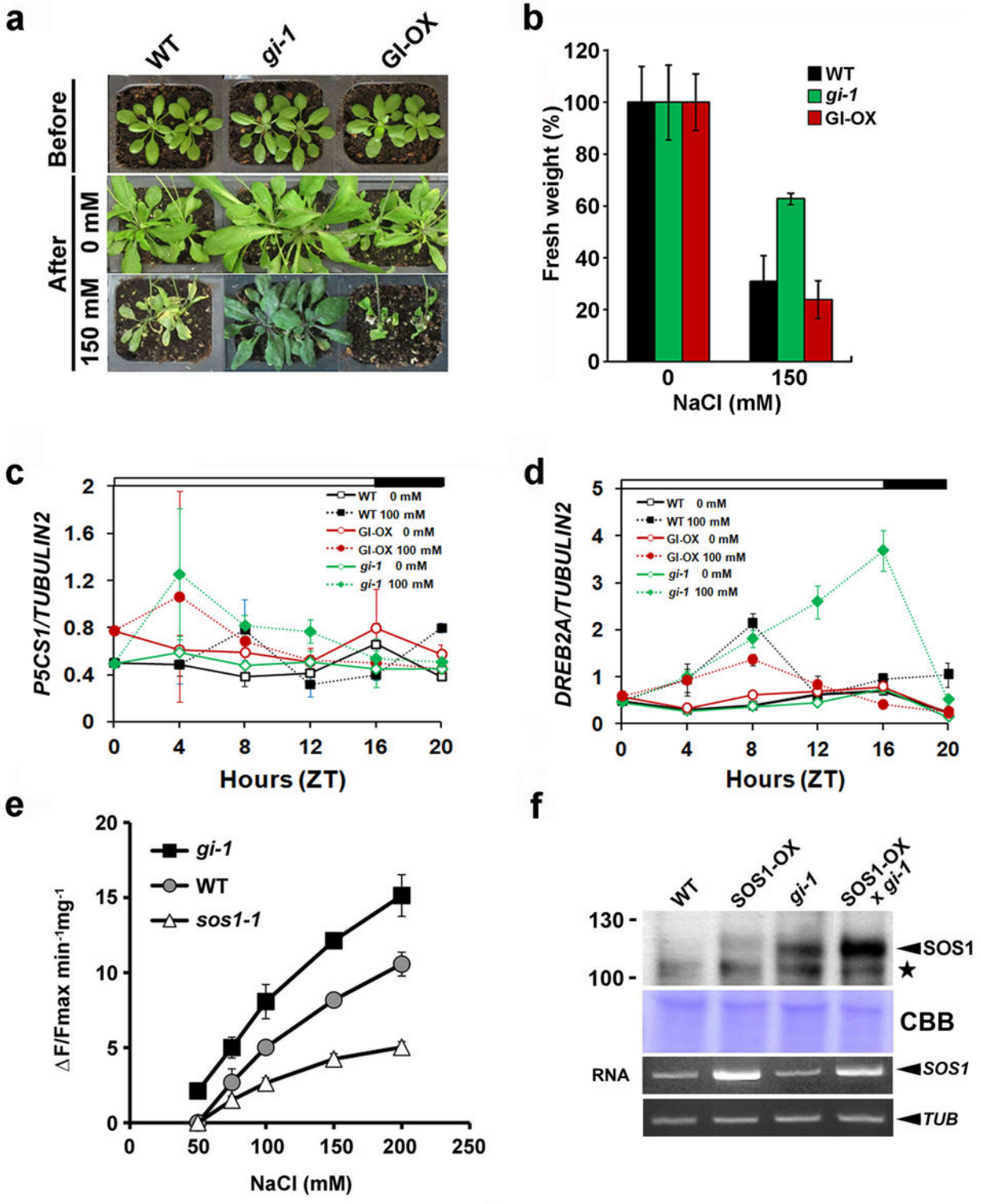
a
WT
gi-1
GI-OX
Before
After
0 mM
150 mM
b
Fresh weight (%)
120
100
80
60
40
20
0
WT
gi-1
GI-OX
0
150
NaCl (mM)
c
P5CS1/TUBULIN2
2
1.6
1.2
0.8
0.4
0
WT 0 mM
WT 100 mM
GI-OX 0 mM
GI-OX 100 mM
gi-1 0 mM
gi-1 100 mM
0
4
8
12
16
20
Hours (ZT)
d
DREB2A/TUBULIN2
5
4
3
2
1
0
WT 0 mM
WT 100 mM
GI-OX 0 mM
GI-OX 100 mM
gi-1 0 mM
gi-1 100 mM
0
4
8
12
16
20
Hours (ZT)
e
ΔF/Fmax min-1mg-1
20
15
10
5
0
gi-1
WT
sos1-1
0
50
100
150
200
250
NaCl (mM)
f
WT
SOS1-OX
gi-1
SOS1-OX x gi-1
130 -
100 -
SOS1
★
CBB
RNA
SOS1
TUB

Figure 2

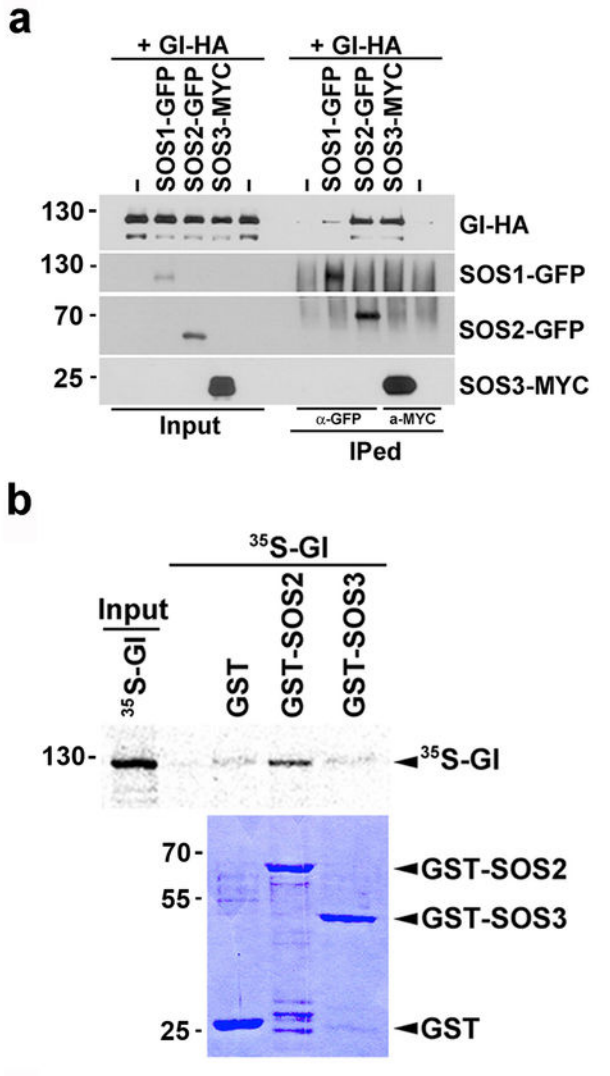
a
+ GI-HA
+ GI-HA
SOS1-GFP
SOS2-GFP
SOS3-MYC
SOS1-GFP
SOS2-GFP
SOS3-MYC
130
130
70
25
GI-HA
SOS1-GFP
SOS2-GFP
SOS3-MYC
Input
α-GFP
a-MYC
IPed
b
35S-GI
Input
35S-GI
GST
GST-SOS2
GST-SOS3
130
35S-GI
70
55
25
GST-SOS2
GST-SOS3
GST
c
-TH
-THU
-THU+FOA
Positive C
Negative C
GI+SOS2
GI+SOS3

Figure 3

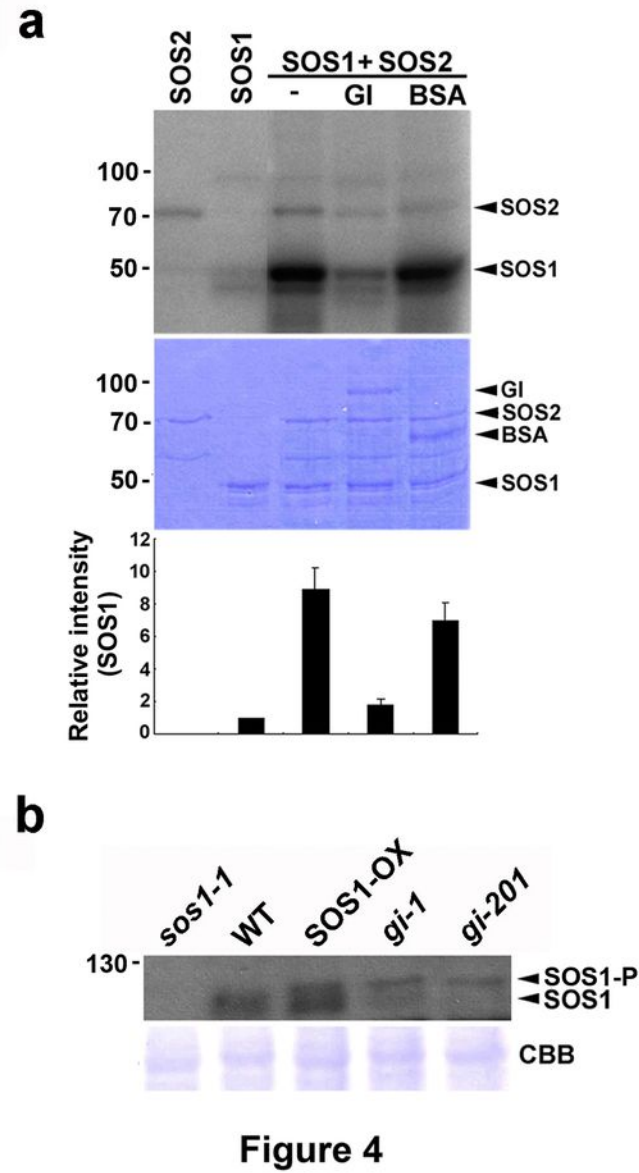
a
SOS2
SOS1
SOS1+SOS2
-
GI
BSA
100
70
50
SOS2
SOS1
GI
BSA
Relative intensity (SOS1)
12
10
8
6
4
2
0
b
sos1-1
WT
SOS1-OX
gi-1
gi-201
130
SOS1-Pi
SOS1
CBB

Figure 4

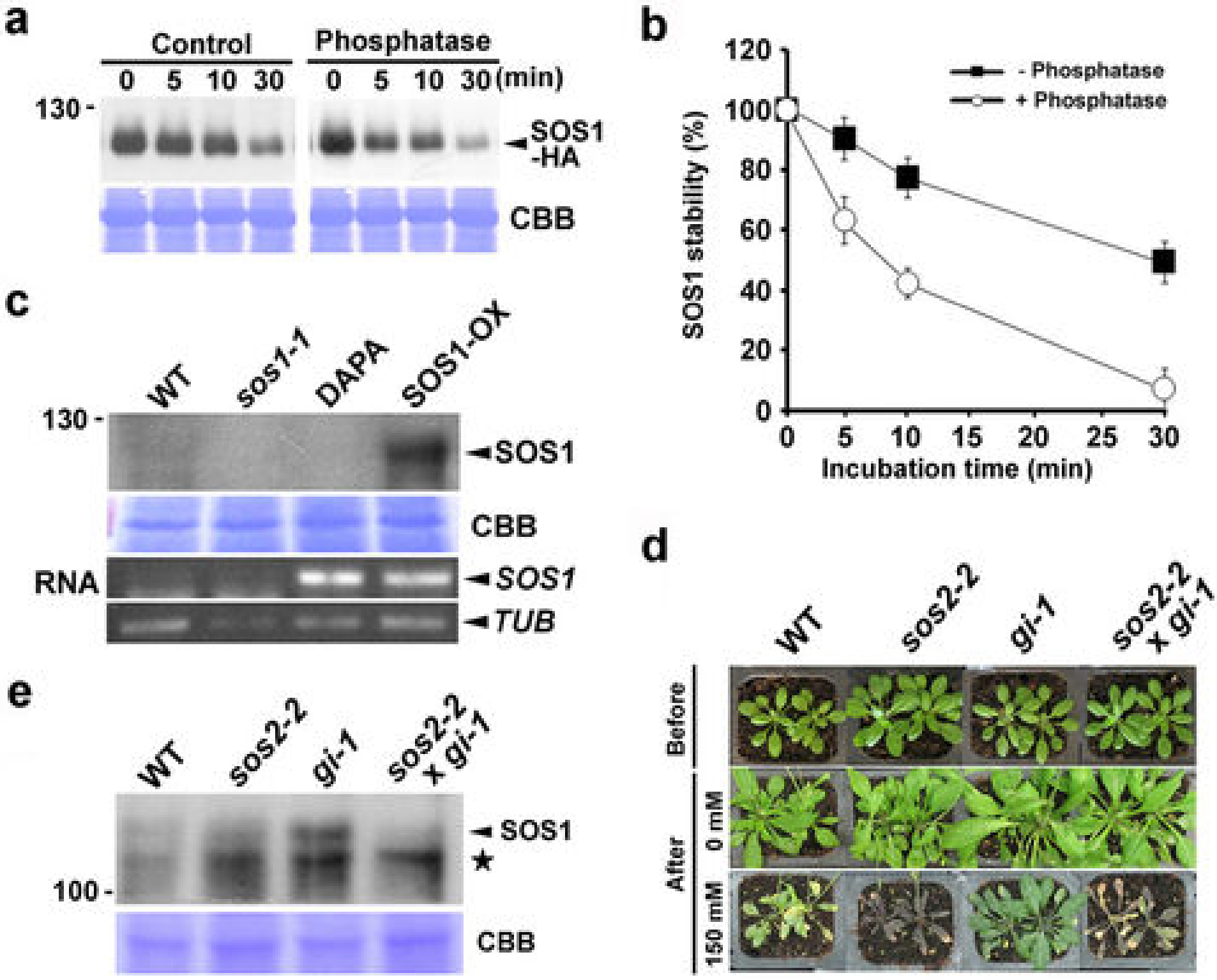
a
Control
Phosphatase
0 5 10 30 0 5 10 30 (min)
130 -
SOS1 -HA
CBB
b
120
100
80
60
40
20
0
SOS1 stability (%)
- Phosphatase
+ Phosphatase
0 5 10 15 20 25 30
Incubation time (min)
c
WT
sos1-1
DAPA
SOS1-OX
130 -
SOS1
CBB
RNA
SOS1
TUB
d
WT
sos2-2
gi-1
sos2-2 x gi-1
Before
After
0 mM
150 mM
e
WT
sos2-2
gi-1
sos2-2 x gi-1
100 -
SOS1
★
CBB

Figure 5

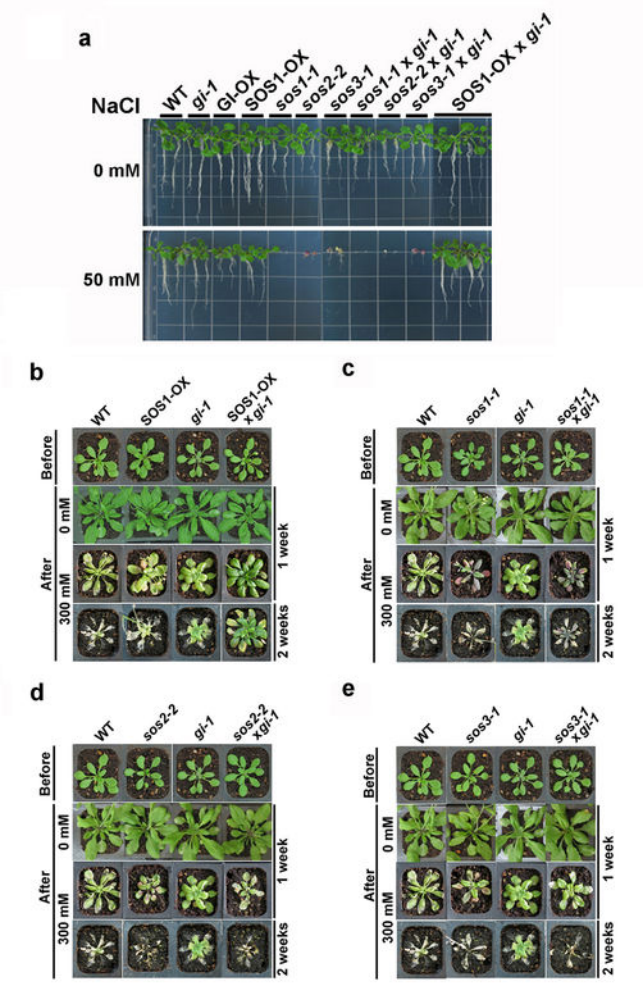
a
NaCl
WT
gi-1
GI-OX
SOS1-OX
sos1-1
sos2-2
sos3-1
sos1-1 x gi-1
sos2-2 x gi-1
sos3-1 x gi-1
SOS1-OX x gi-1
0 mM
50 mM
b
WT
SOS1-OX
gi-1
SOS1-OX x gi-1
Before
After
0 mM
300 mM
1 week
2 weeks
c
WT
sos1-1
gi-1
sos1-1 x gi-1
Before
After
0 mM
300 mM
1 week
2 weeks
d
WT
sos2-2
gi-1
sos2-2 x gi-1
Before
After
0 mM
300 mM
1 week
2 weeks
e
WT
sos3-1
gi-1
sos3-1 x gi-1
Before
After
0 mM
300 mM
1 week
2 weeks

Figure 6

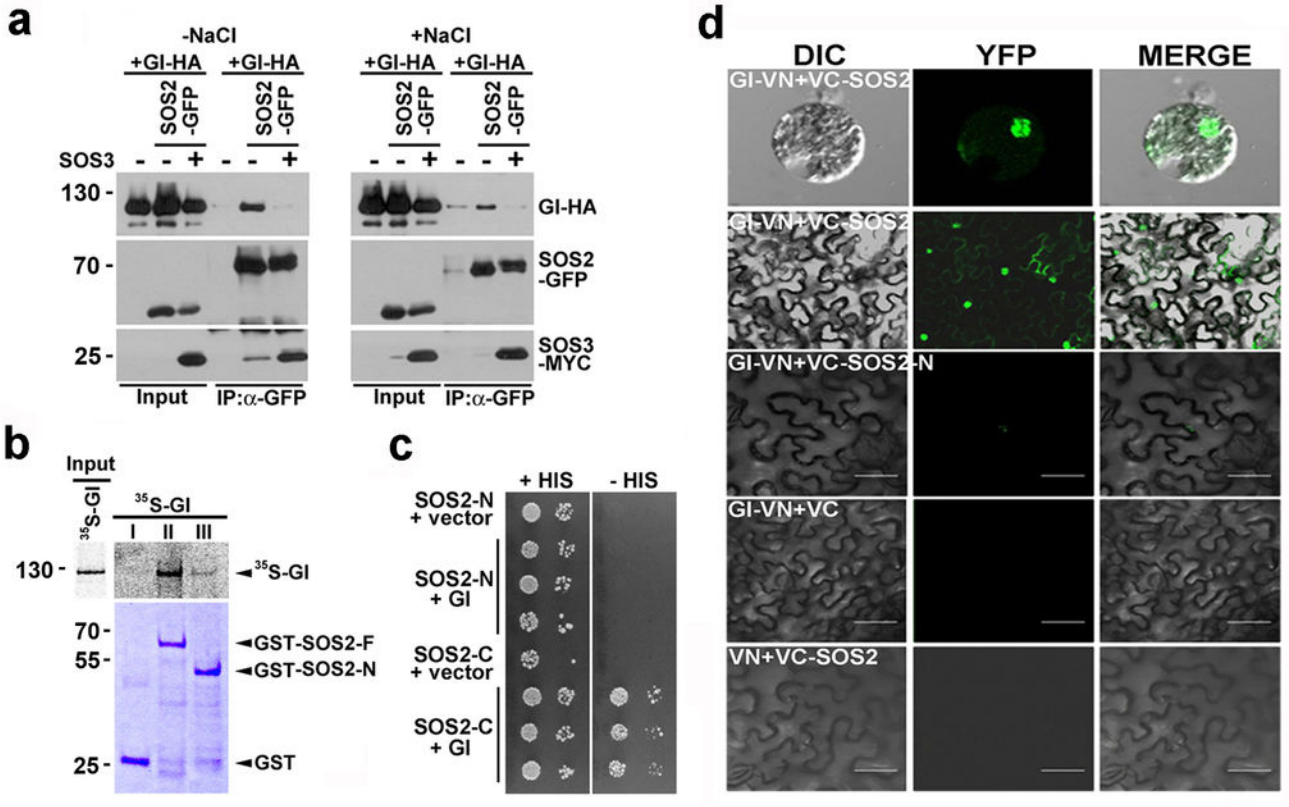
a
-NaCl
+NaCl
+GI-HA
SOS2 -GFP
SOS3
130
70
25
GI-HA
SOS2 -GFP
SOS3 -MYC
Input
IP:α-GFP
b
Input
35S-GI
I
II
III
GST-SOS2-F
GST-SOS2-N
GST
c
+ HIS
- HIS
SOS2-N + vector
SOS2-N + GI
SOS2-C + vector
SOS2-C + GI
d
DIC
YFP
MERGE
GI-VN+VC-SOS2
GI-VN+VC-SOS2-N
GI-VN+VC
VN+VC-SOS2

Figure 7

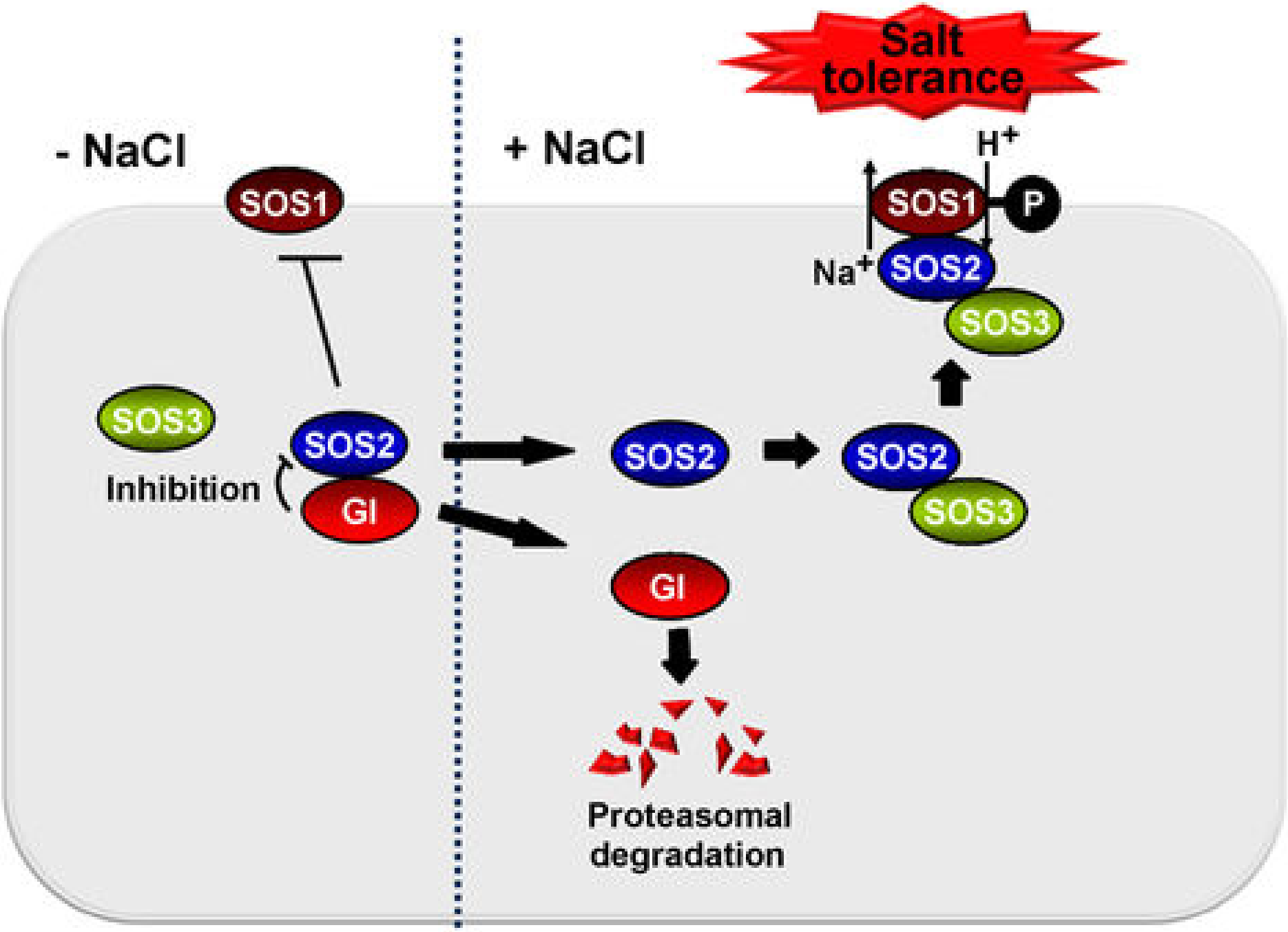
Salt tolerance
- NaCl
+ NaCl
SOS1
SOS3
SOS2
Inhibition
GI
SOS2
GI
Proteasomal degradation
H+
SOS1
P
Na+
SOS2
SOS3
SOS2
SOS3

Figure 8

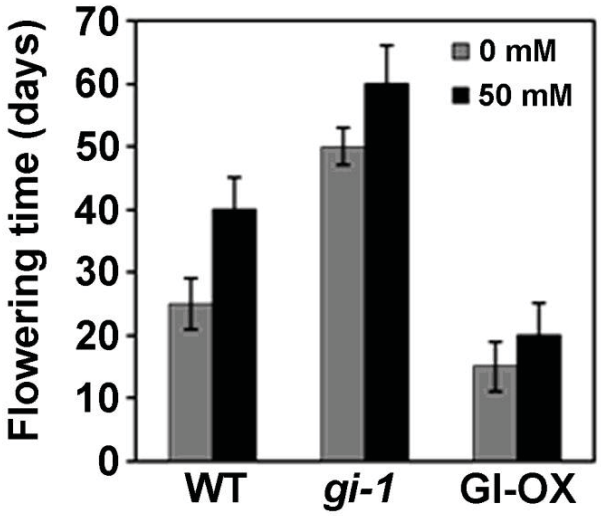

Supplementary Figure S1. Salt treatments delay flowering in *Arabidopsis*.

Days to bolting of WT, *gi-1,* and GI-OX (*35S::GI-HA*) plants grown under long-day conditions (16 h light/8 h dark) on basal medium containing 1% agar without or with 50 mM NaCl supplement. Mean ± SE of flowering time are shown (n=12).

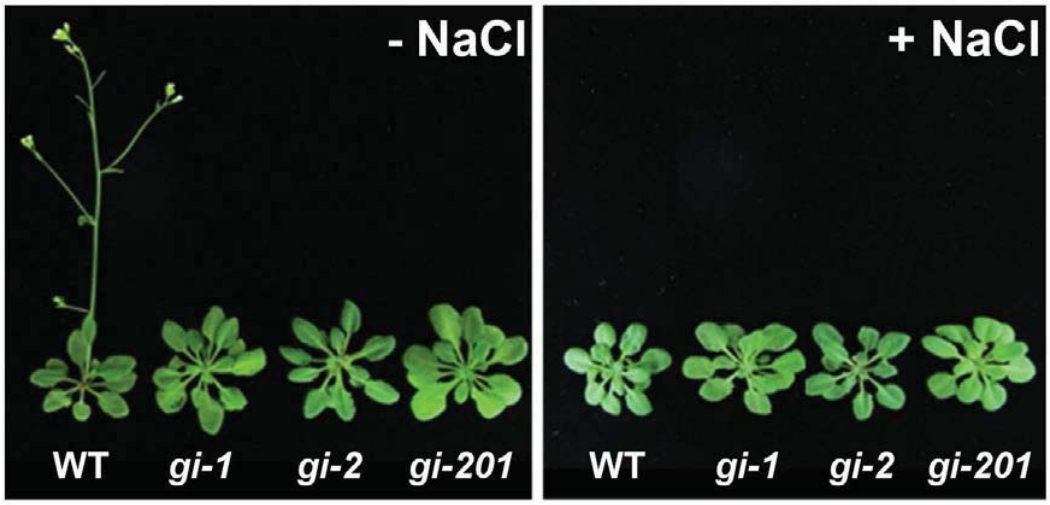

Supplementary Figure S2. GI is required for salt-induced delay of flowering in *Arabidopsis*.

Shown are five-week-old WT, *gi-1, gi-2* and *gi-201* plants grown under long-day conditions (16 h light / 8 h dark) on basal medium containing 1% agar without (-NaCl) or with (+NaCl) 50 mM NaCl supplement.

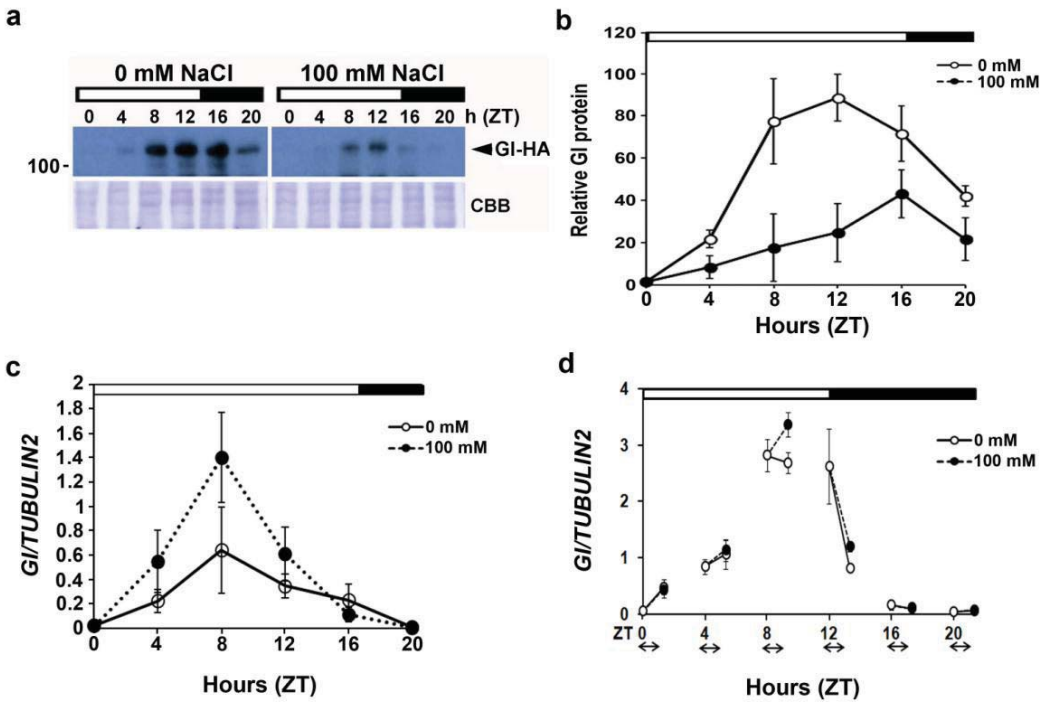

Supplementary Figure S3. Diurnal cycling of *GI* transcript and GI protein levels in untreated and salt-treated plants.

Two-week-old plants [GI:GI-HA] grown under long-day conditions (16 h light/8 h dark) on basal medium were treated with 0 mM or 100 mM NaCl at ZT0 and harvested every four hours thereafter, i.e., with the time of salt treatment as in Figure 1C. (a) GI protein was detected in total protein extracts by immunoblotting using an anti-HA antibody. The Coomassie (CBB) stained gel is shown as loading control. Molecular weight markers in kDa. (b) Quantification of GI-HA protein on the immunoblots. Values are expressed relative to intensity of CBB-stain. (c) Transcript levels of *GI* were measured by real-time PCR and normalized to the transcript level of *TUBULIN2*. Data represent the average of three independent experiments ± SE. The white-and-black bar along the x-axis indicates light and dark periods, respectively. (d) Total RNA was extracted from ten day-old seedlings of WT plants that were grown under 12 h light/12 h dark conditions in basal medium and treated without (solid line) or with (dotted line) 100 mM NaCl at ZT0, 4, 8, 12, 16, and 20. Transcript levels were measured by qRT-PCR before and 1 h after salt treatment (indicated by arrows). *TUBULIN2* was used for normalization. Data represent mean ± SE of three biological repeats with 2 technical repeats each (n=3).

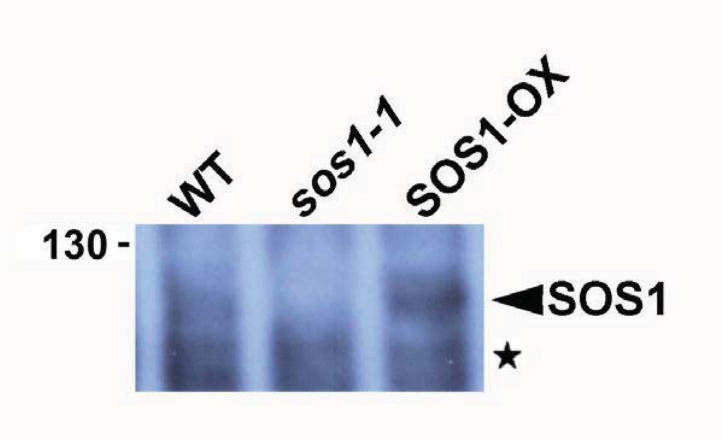

Supplementary Figure S4. Anti-SOS1 antibody detects SOS1 *in vivo*.

Detached leaves of WT, *sos1-1*, and SOS1-OX plants were treated with 100 mM NaCl for 24 h. Total protein extracts were subjected to immunoblot analysis using anti-SOS1 antibody. Asterisk indicates position of nonspecific cross-reacting band. Arrowhead indicates SOS1 position. Molecular weight markers in kDa.

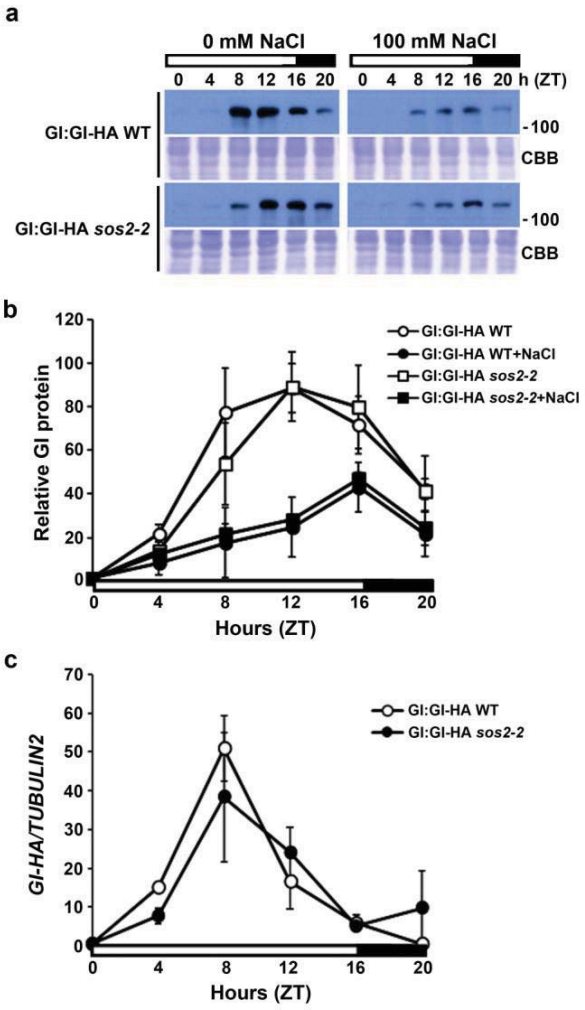

Supplementary Figure S5. Comparison of diurnal cycling of GI protein and mRNA levels in salt-treated and untreated WT and *sos2-2* plants.

Two-week-old plants expressing HA-tagged GI from the *GI* promoter (*GI:GI-HA*) in the WT and *sos2-2* background were treated with 100 mM NaCl at ZT0 and harvested thereafter at four hour intervals. (a) Comparison of GI protein levels. GI-HA protein was detected on immunoblots using an anti-HA antibody. The CBB-stained bands are shown as loading control. Molecular weight markers in kDa. (b) Quantitative representation of the data shown in (a). GI-HA protein was quantified relative to intensity of CBB-stain. Horizontal white-and-black bars represent light and dark period, respectively. (c) Transcript levels of *GI* were measured by real-time PCR and normalized to the transcript level of *TUBULIN2*. Data represent the average of three independent experiments ± SE. The white-and-black bar along the X-axis indicates light and dark periods, respectively.

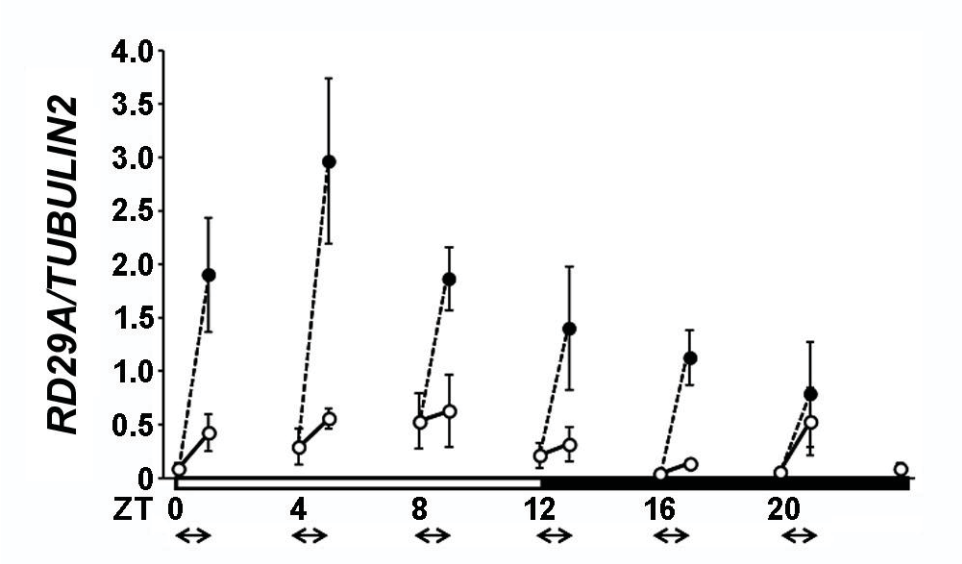

Supplementary Figure S6. *RD29A* transcripts are most strongly induced by salt during the early part of the day. Total RNA was extracted from ten day-old seedlings of WT plants that were grown under 12 h light/12 h dark conditions in basal medium and treated without (solid line) or with (dotted line) 100 mM NaCl at ZT0, 4, 8, 12, 16, and 20. Transcript levels were measured by qRT-PCR before and 1 h after salt treatment (indicated by arrows). *TUBULIN2* was used for normalization. Data represent mean ± SE of three biological repeats with 2 technical repeats each (n=3).

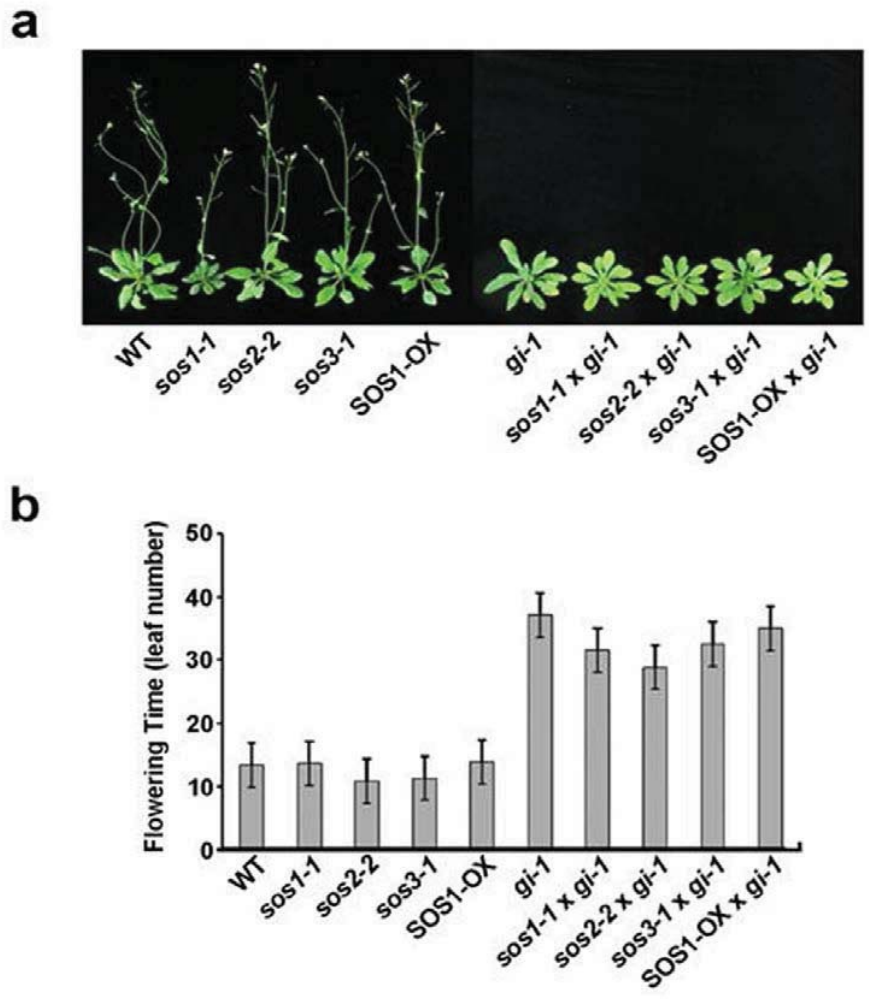

Supplementary Figure S7. Flowering time is not controlled by the SOS pathway genes.

(a) Plants of indicated lines were grown in basal medium containing 1% agar under 16 h light / 8 h dark conditions and photographed after 27 days. (b) Flowering time of these plants was measured as total number of leaves (rosette + cauline) produced at bolting. Data represent mean ± SE (n>15). Symbol: SOS1-OX, *35S:SOS1*.

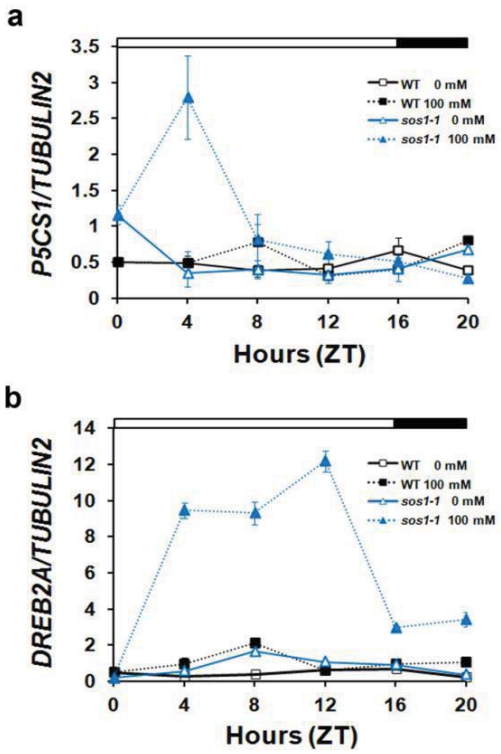

Supplementary Figure S8. *P5CS1* and *DREB2A* transcript levels were dramatically changed in *sos1-1*.

qRT-PCR analysis of *P5CS1* (a) and *DREB2A* (b) transcript levels over 20 h NaCl treatment. Ten-day-old seedlings were treated with (dotted line) or without (solid line) 100 mM NaCl at ZT0. *TUBULIN2 (TUB2*) was used as internal control. Data represent the mean ± SE of three independent experiments. White-and-black bar represents light and dark periods, respectively.

Supplementary Table S1. Primers used for plasmid construction and PCR.

Primer	Sequence	Purpose
GI-RT-f	CTGTCTTTCTCCGTTGTTTCACTGT	RT-PCR and Real-time PCR
GI-RT-r	TCATTCCGTTCTTCTCTGTTGTTGG	RT-PCR and Real-time PCR
SOS1(1281)-f	CGTGAAGCAATCAAGCGGAAATT	RT-PCR
SOS1(1398)-r	AAATTGGGTAGTGGATCCATTAAC	RT-PCR
TuB-F(qRT)	TGGCATCAACTTTCATTGGA	RT-PCR
TuB-R(qRT)	ATGTTGCTCTCCGCTTCTGT	RT-PCR
GST-SOS1C-f	CGCGGATCCCCGTTCTACGCCTTCTTCGCATG G	Plasmid construction
GST-SOS1C-r	ACGCGTCGACTAGATCGTTCCTGAAAACGATT	Plasmid construction
GST-SOS2-f	CGCGGATCCATGACAAAGAAAATG	Plasmid construction
GST-SOS2-r	ACGGTCGACTCAAAACGTGATTGTTCTGAG	Plasmid construction
GST-SOS2/268- r	ACGGTCGACTCAATAATTTAATCTGAACCAAGG	Plasmid construction
GST-SOS2/308- r	ACGCGTCGACTCACAGGGGCCCTTCATCATTT C	Plasmid construction
GST-SOS2/329- r	ACGCGTCGACTCAGTCAAATAGTGCAGATAAAT	Plasmid construction
GI-f(pTriEX)	GGATCCGATGGCTAGTTCATCTTC	*In vitro* binding assay
GI-r(pTriEX)	GGTACCATTGGGACAAGGATATAG	*In vitro* binding assay
SOS2-GW-f-p	AAAAAGCAGGCTTCATGACAAAGAAAATGAGAA G	BIFC and yeast two hybrid
SOS2-GW-r (with stop codon)	AGAAAGCTGGGT*TCA*AAACGTGATTGTTCTGAG	BIFC and yeast two hybrid

SOS2-GW-r (without stop codon)	AGAAAGCTGGGTCAAACGTGATTGTTCTGAGAA T	BIFC
SOS3-GW-f	AAAAAGCAGGCTTCATGGGCTGCTCTGTATCGA A	BIFC, GST-SOS3 and yeast two hybrid
SOS3-GW-r (with stop codon)	AGAAAGCTGGGTC*TTA*GGAAGATACGTTTTGCA AT	BIFC, GST-SOS3 and yeast two hybrid
SOS3-GW-r (without stop codon)	AGAAAGCTGGGTCGGAAGATACGTTTTGCAAT	BIFC
attB1 adapter	GGGGACAAGTTTGTACAAAAAAGCAGGCT	Gateway
attB2 adapter	GGGGACCACTTTGTACAAGAAAGCTGGGT	Gateway
CO(qRT)5	ATTCTGCAAACCCACTTGCT	Real-time PCR
CO(qRT)3	CCTCCTTGGCATCCTTATCA	Real-time PCR
FT(qRT)F	CTGGAACAACCTTTGGCAAT	Real-time PCR
FT(qRT)R	AGCCACTCTCCCTCTGACAA	Real-time PCR
P5CS(qRT)-F	AGCAGCCTGTAATGCGATGG	Real-time PCR
P5CS(qRT)-R	AAGTGACGCCTTTGGTTTGC	Real-time PCR
DREB2A(qRT)-F	CTGGAGAATGGTGCGGAAGA	Real-time PCR
DREB2A(qRT)- R	CAGATAGCGAATCCTGCTGTTGT	Real-time PCR
RD29A(qRT)-F	ATCACTTGGCTCCACTGTTGTTC	Real-time PCR
RD29A(qRT)-R	ACAAAACACACATAAACATCCAAAGT	Real-time PCR
TUBULIN2(qRT)-F	AGCAAATGTGGGACTCCAAG	Real-time PCR
TUBULIN2 (qRT)-R	CACCTTCTTCATCCGCAGTT	Real-time PCR
Actin(qRT)-F	TATCGCTGACCGTATGAGCAAAG	Real-time PCR
Actin(qRT)-R	TGGACCTGCCTCATCATACTCG	Real-time PCR

Supplementary Methods

Cloning. For recombinant protein expression, the SOS1 C-terminal fragment (SOS1 CD3; 885-1146 aa), full-length SOS2 (SOS2-F, 1–446 aa), $SOS2^{T168D}$ that has constitutively activated SOS3-independent kinase activity[35], SOS2 N-terminal fragment (SOS2-N, 1-308 aa) and full-length SOS3 were amplified with *Pfu* DNA polymerase (Solgent) using the primer pairs described in Supplementary Table S1. The PCR products were cloned into *pGEX-5X-3* (SOS1 CD3), *pGEX-2T* (SOS2s), and *pGEX-4T-3* (SOS3) to generate in-frame GST fusions. GI N-terminal fragment[27], (GIN, amino acids 1-391) was subcloned into the *pGEM-T* easy vector (Promega), and then inserted into *pIH1119* (NEB) between the *BamH*I and *Not*I site s to generate the in-frame MBP-GIN fusion construct.

For *in vitro* binding assays, the full-length ORF of GI was cloned into *pTriEX-1* vector (Novagen). For BiFC, full-length ORF sequences for SOS2 were amplified with indicated primers (Supplementary Table S1) to generate entry vectors [SOS2 with or without stop codons in the *pDONR^{TM}/Zeo* vector (Invitrogen)]. The *GI* entry vector, *pENTR-1A-Amp-GI(s)*, was a kind gift from Dr. Nam. SOS2 and GI were fused in-frame to Venus aa 1-173 and Venus aa 156-239, which contained the N- and C-terminal fragments of the eYFP fluorescent protein in the *pDEST-VYNE(R)^{GW}* and *pDEST-VYCE(R)^{GW}* vectors, respectively[54]. For the yeast split-ubiquitin assay, *GI* was cloned into *pMet-GWY-Cub-RUra3*, and *SOS2* and *SOS3* were cloned into *pCup-NuI-GWY*. For the yeast two-hybrid assay, full-length *GI* ORF was cloned in the yeast two-hybrid activation domain vector *pACT2* (Clontech). *SOS2* ORF fragments, encoding either the catalytic N-terminal domain (SOS2-N, 1 to 308 aa) or the regulatory C-terminal domain (SOS2-C, 309 to 446 aa), were cloned in the binding domain vector *pAS2.1*.

Preparation of recombinant proteins. The recombinant proteins GST-SOS1 CD3 and MBP-GIN(1-391) were expressed in *Escherichia coli* BL21 (DE3) pLysS. GST-SOS2 proteins and GST- SOS3 were expressed in *E. coli* BL21 (DE3). Because It is very difficult to purify intact forms of GI full length protein as a recombinant protein, we used minimal length of GI protein (1-391aa) which has known to be enough to interact with other interactors[23,33]. Protein expression was induced by the addition of 0.5 mM isopropyl-1-thio-β-$_D$-gal-actopyranoside (IPTG) for 4 h at 30℃ (GST-SOS1 CD3), 1 mM (IPTG) for 16 h at 16℃ (GST-SOS2s) or for 4 h at 30℃ (for GST-SOS3 and MBP-GIN). To isolate GST-SOS proteins, cells were disrupted by sonication with 1% Triton X-100 and 1 mM DTT and purified using glutathione-cellulose affinity chromatography (Bioprogen). The cells expressing MBP-GIN were suspended in 1X PBS with protease inhibitors (1 mM PMSF, 5 μg/ml leupeptin, 1 μg/ml aprotinin A, and 1 μg/ml pepstatin), 1 mM DTT and 1% Triton X-100 and disrupted by sonication. MBP-GIN was purified by affinity chromatography using amylose resin (NEB) and eluted with 20 mM maltose.

Supplementary Reference

54. Gehl, C., Waadt, R., Kudla, J., Mendel, R.-R. & Hansch, R. New GATEWAY vectors for high throughput analyses of protein-protein interactions by bimolecular fluorescence complementation. *Mol. Plant* 2, 1051-1058 (2009).